MISSOURI S&T | CURTIS LAWS WILSON LIBRARY
MISSOURI UNIVERSITY OF SCIENCE AND TECHNOLOGY

Scholars' Mine

Masters Theses | Student Theses and Dissertations

1962

A model study of the induction log applied to the detection of asymmetrically located orebodies

Robert Walter Piekarz

Follow this and additional works at: https://scholarsmine.mst.edu/masters_theses

 Part of the Mining Engineering Commons

Department:

Recommended Citation

Piekarz, Robert Walter, "A model study of the induction log applied to the detection of asymmetrically located orebodies" (1962). *Masters Theses*. 4167.
https://scholarsmine.mst.edu/masters_theses/4167

This thesis is brought to you by Scholars' Mine, a service of the Curtis Laws Wilson Library at Missouri University of Science and Technology. This work is protected by U. S. Copyright Law. Unauthorized use including reproduction for redistribution requires the permission of the copyright holder. For more information, please contact scholarsmine@mst.edu.

www.manaraa.com

T1401

H6059

A MODEL STUDY OF THE INDUCTION LOG APPLIED TO THE DETECTION OF ASYMMETRICALLY LOCATED OREBODIES

BY

ROBERT WALTER PIEKARZ

A

THESIS

submitted to the faculty of the

SCHOOL OF MINES AND METALLURGY OF THE UNIVERSITY OF MISSOURI

in partial fulfillment of the work required for the

Degree of

MASTER OF SCIENCE IN MINING ENGINEERING

Rolla, Missouri

1962

MISSOURI SCHOOL OF MINES & M.T. LIBRARY 1045 80 OCT 8 1962 PROPERTY ROLLA, MO.

Approved by

(Advisor)

Gerard B. Rupert

Paul Dean Proctor

ABSTRACT

This research project was undertaken to determine the possibility of using an induction log of the type applied in petroleum exploration, for the detection of conductive ore-bodies asymmetrically located with respect to a borehole. Since a mathematical analysis would be extremely complex, a model study was conducted, using graphite bodies of various shapes to simulate different modes of mineral occurance.

The investigation showed that these bodies were readily detectable, and were capable of yielding anomalous curves characteristic of their geometry. The values of apparent conductivity decreased rapidly with lateral displacement, from the logging tool, as expected, due to the resistive air medium.

ACKNOWLEDGEMENTS

The author wishes to express his sincerest appreciation to Dr. H. M. Zenor for his help in the selection of this thesis subject and for his guidance, help and constructive criticism through the major portion of the investigation.

Special thanks are due to the Lane Wells Company for their financial assistance, and for permission to use their research data prior to its publication date.

Thanks are also due Professor J. P. Govier, Chairman of the Department of Mining Engineering for making available the use of the Mining Department facilities during the study.

TABLE OF CONTENTS

LIST OF FIGURES

LIST OF TABLES

I. INTRODUCTION

One of the many factors so essential to the success of any mining venture is the knowledge of the orebody location, size, and grade. Much of this knowledge is gained through the analysis of diamond drill cores, drill cuttings, sludge, and recently through borehole geophysics. However, borehole geophysics, as applied to underground and surface mining exploration is still in its embryo stages. In the few instances where electric logging methods have been applied, the results were good, showing indications of further promise.

Due to the variable directional aspects and small sizes of mining boreholes, many electric logging tools must be discarded in favor of a small diameter device capable of wet and dry hole operation. Such a device is the induction log. Many orebodies, especially the sulfides, may render themselves detectable by induction logging techniques by nature of their inherent high electrical conductivities.

This concept could supplement many of the existing mineral exploration methods, especially where difficult core or sludge recovery conditions are experienced, or where cost considerations merit other techniques. The economy of percussive long hole drilling coupled with the information supplied by an induction logging device certainly merits investigation.

The quantitative aspects of this tool in petroleum exploration have been facilitated by the fact that the zones

of investigation are generally bedded and are assumed perpendicular to the borehole axis. This concept permits a mathematical analysis from symmetrical considerations; i.e., cylindrical or disklike methods generally apply.

Orebodies, however, are oriented in a haphazard way, nearly always asymmetrical to any borehole axis that passes through them, if intersected at all. Since the shape of orebodies is so variable;i.e., veins, pipes, lenses, masses, etc., mathematical considerations are extremely complex. The preferred approach then, is through a model study, supplemented by mathematical considerations where applicable.

The purpose of this study is to determine the applicability of the induction log in detecting orebodies asymmetrically located with respect to the borehole.

Investigations consisted of a model study of the effects in air of graphite cylinders, prisms, slabs, and composite bodies on a two coil model induction logging tool located at varying distances parallel, perpendicular, or skew to the bodies. Graphite was chosen because its scale conductivity is compatible with that of certain highly conductive sulfide ore minerals. The results of the investigation are presented in section IV of this dissertation.

Tabulated values of apparent conductivities to be expected in typical host rocks are discussed in section VII.

II. REVIEW OF LITERATURE

A. Theoretical

"Induction logging is a method which measures the conductivity (reciprocal of resistivity) of formations by means of induced alternating currents. . ." Schlumberger, Document 8, (1958, p. 37). Since this is an induction method, insulated coils are used to energize the formations and the borehole can contain "any fluid, water base mud, oil-base mud, gas or air" Schlumberger Document 8, (1958, p. 37).

> According to Doll (1949, p. 3) "The induction logging system does not require any direct contact with the ground. . . alternating current of the appropriate frequency [20,000 cps] is made to flow through a coil, referred to as a 'transmitter' which is supported by an insulating mandrel. The alternating magnetic field thus generates eddy currents [Foucault currents] which. . . follow circular paths, coaxial with the coil system and the hole, in the formations surrounding said hole. These eddy currents create a secondary magnetic field which induces an electromotive force in a second coil, referred to as a 'receiver', mounted on the same nonconductive mandrel at a certain distance [generally 40 inches] called 'spacing', from the transmitter."

> "If the transmitter current is maintained at a constant value, the intensity of the eddy current is proportional to the conductivity of the ground. Thereby, the conductivity of the ground determines the secondary field created by the eddy currents, and the signal generated in the receiver."

In his mathematical treatment of this concept, Doll, (1949, p. 6) assumes the borehole to be vertical; i. e., normal to the beds so that the lines of current flow are horizontal circumferences, concentrically located with respect to the borehole axis. He also requires a symmetry of

revolution so that ". . . each line of current flow remains in the same medium all along its path, and never crosses a boundary between media of different conductivities," and assumes the coil dimensions are an insignificant factor when compared to the diameter of the ground loop whose influence it is proposed to determine. His work was done with the assumption that the interaction of the eddy currents on each other, or "skin effect" is negligible provided that the frequency is not too high. The concepts of "unit ground loop" and "geometrical factor" are utilized in his paper.

> Doll (1949, p. 7) defines the unit ground loop as ". . . by definition. . . a horizontal loop of homogeneous ground, having a circular shape with its center on the axis of the hole, and whose cross section is a very small square of unit area," and the geometrical factor of the ground loop ". . . the fraction of the total signal contributed by such section."

Figure 1 illustrates these premises.

A series of interpretative charts, based on the forementioned concepts are published by the Schlumberger Well Surveying Corporation (Schlumberger Document 2, 1958) applicable to qualitative and quantitative induction log curve interpretation for the petroleum industry.

Dumanoir, Tixier, and Martin (1957) have published curves of induction log systems with "skin effect" considered, but no information regarding the accounting of these effects is given.

Consideration to the propagation of eddy currents or "skin effect" is given by Duesterhoeft (1961, p. 193-204)

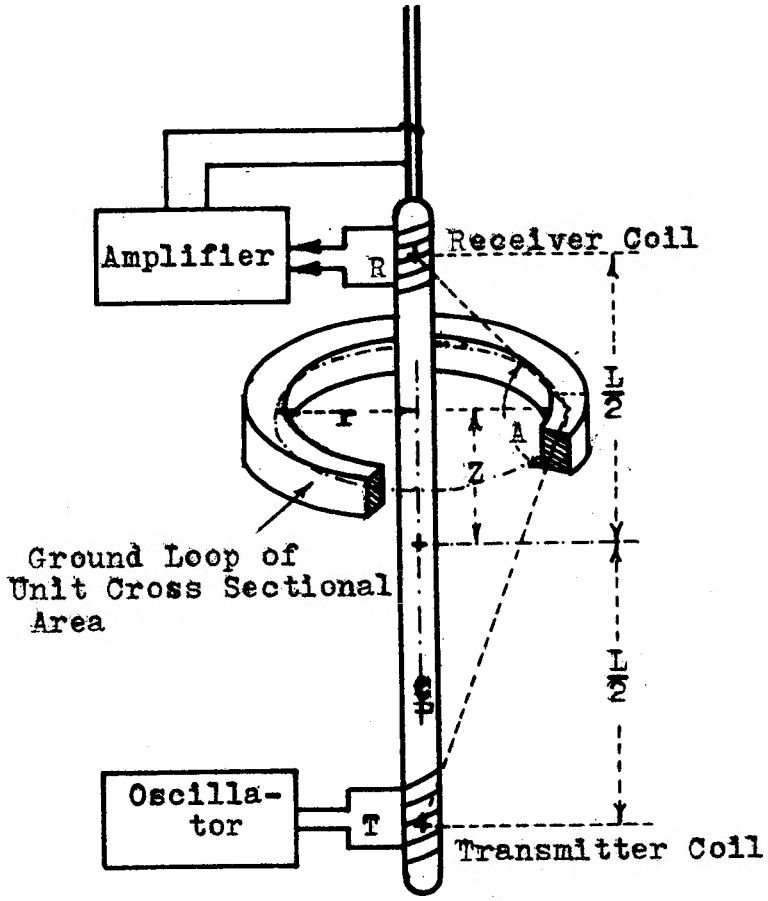

Z = Distance of center of ground loop from center of coil system.

A = Angle subtended by groundloop in respect to coils.

r = Radius of ground loop.

$\sin^3 A$ = Geometrical factor.

Fig. 1 Schematic, Illustrating the Concept of Unit Ground Loop and the Geometrical Factor of a Two Coil Induction Log

(After Doll, 1949)

in his studies of the induction log located in a homogeneous medium, near a horizontal interface, and in a bedded layer.

> Duesterhoeft (1961, p. 193) in his analysis of the induction log states, "a regulated alternating current in the transmitter coil induces current flow in the earthen formation surrounding the borehole. This eddy current is approximately in phase-quadrature with the transmitter current. The earth currents in turn induce a voltage in the receiver coil that is in phase-quadrature with the earth currents and, hence, in phase with the transmitter current. . . The measurement of conductivity is accomplished by phase discrimination in the receiver."

He shows through analysis of the vector field equations that the receiver voltage is composed of voltage components due to mutual inductance, formation conductivity, and propagation or "skin effect". The mutual inductance component is removed via phase discrimination in the receiver and the in-phase component is determined by phase sensitive detection. Again, Duesterhoeft assumes symmetry of revolution in his analysis as does Doll.

Zenor and Oshry (1962, in a research whose results are to be published postdating this writing) prove by utilizing the techniques of circuit theory, that the concept of geometrical factor is modified by the propagation effect or "skin effect". Their work, programmed on the Royal McBee LPG 30 Digital Computer at the Missouri School of Mines Computer Center and the IBM 1090 at CEIR, Houston, Texas, gives the modification of the geometrical factor due to skin effect for each ground loop and the modification to the receiver voltage. In their report (1962) they state,". . . This method is

usable for the most complicated of axially symmetrical ground configurations".

In personal communication, Zenor (1962) stated ". . . that for the complexities of asymmetrical considerations of the induction log. . . reliance can be placed on model studies."

B. Applied

Heiland (1946) discusses inductive methods of exploration through the use of horizontal and vertical coils on the surface of the ground.

Seigel (1952) solved the problem of size determination of oblate spheroidal shaped sulfide orebodies by using a three electrode resistivity apparatus in a borehole. The major axis of the oblate spheroid was normal to the borehole. The borehole axis bisected the orebody, and a mathematical analysis using oblate spheroidal coordinates was effected. It was interesting to note Seigel's remark (1952, p. 907) concerning . . . "a factor of 1000-fold contrast in electrical conductivities of the sulphide and country rock".

Clark (1956) conducted an investigation of prolate spheroidal shaped sulfide orebodies in Canada using borehole resistivity apparatus. This method required actual contact with the orebody with one electrode and utilizing the other electrode at the earth's surface. Through the use of this method, he was able to delineate the long axis of the orebody. Although Clark's method has little application to this

investigation, it does represent an effort to delineate an orebody asymmetrically located with respect to the borehole axis.

Boyum (1957) discusses the results of logging small diameter drill holes in the Marquette Iron Range by the Schlumberger Company. Although only resistivity methods were applied, virtually all formation contacts were detected, and pronounced differences in resistivity between the iron formation and intrusives were noted. In general, the oxidized iron formations ranged from 20-100 ohm-meters resistivity, and the intrusive material ranged from 100-900 ohm-meters resistivity.

Hallof (1957) discusses an electromagnetic method where a receiver coil, located in a borehole, is energized from the effects of a large transmitter coil located at the surface. Measurements are taken at 100 foot intervals, and the resulting curve is compared to those of past experience and scale model experiments.

> Hallof (1957,p. 12) states that . . ."the magnitude and character of the anomaly caused by a particular conductor [sulfide orebody] . . . depend on the following factors. . . depth of conductor, conductivity of mineralization, shape of conductor, altitude of conductor, distance of conductor from the hole. . ."

The equipment is mobile, but in order to survey a 2000 foot hole one full day is required.

Zablocki and Keller (1957) claim borehole geophysical methods can supplement data from analysis of diamond drill cores in cases of poor core recovery or when borehole samples

are statistically inadequate. They believe the inhole logging device has the advantage of sampling a larger volume than a core, a factor worthy of consideration in disseminated deposits. In the application of the induction logging to the Gogebic Iron Range, holes logged showed marked conductivity highs due to magnetite and hematite, and conductivity lows in the presence of silicate and carbonate formations. All applications of the induction log in the Lake Superior District were in bedded deposits. Moore (1957, p. 31) states ". . . this device [induction log] offers a great deal of promise as a survey tool in mining drill hole exploration".

III. SCALE CONSIDERATIONS

Since there is no "standard" induction logging device in the mining industry, it appears that the equipment precedent established by the petroleum industry in the application of the induction log should be followed as a guide in scale considerations.

A standard two coil tool (non-focussing) was chosen as the prototype because of its comparative simplicity in manipulation and operation as compared to the more complex four and six coil tools of the focussing variety. In this paper, a non-focussing device will incorporate only two coils; i.e., a transmitter coil and a receiver coil, a standard tool used in petroleum exploration. In order to eliminate the circuitry problems of a high frequency model, a frequency of 2000 cps was considered feasible. A 1 to 10 physical size ratio; i.e., a 4" coil spacing was chosen for manipulative ease.

Using the following equation of electrical similitude from Zenor and Oshry (1962) . . .

$$\frac{\sqrt{2\pi f_m \mu_m \sigma_m}}{2} R_m = \frac{\sqrt{2\pi f_e \mu_e \sigma_e}}{2} R_e$$

where

f_m = the frequency in the model

f_e = the frequency in the earth

μ_m = the permeability of the model (generally taken as that of free space)

μ_e = the permeability of the earth (generally taken as that of free space.)

σ_m = the conductivity of the model material

σ_e = the conductivity of the earth material

R_m = main coil spacing of the model tool

R_e = main coil spacing of the earth (full sized)

Solving for σ_m

$$\sigma_m = \frac{f_e}{f_m}\left(\frac{R_e}{R_m}\right)^2 \sigma_e$$

Or, for a model with a tool of 4" spacing and a frequency of 2000 cps, compared to an earth model with a tool of 40" spacing and a frequency of 20KC

$$\sigma_m = 1000\,\sigma_e$$

Therefore, for this model study, any material representing a sulfide mineral should have a conductivity equivalent to one thousand times that of the sulfide mineral. The minerals and the conductivities simulated in this investigation are tabulated in Table I, modified from Jakosky (1960, p. 441). Bornite is considered below as an example of the modification to Jakosky's table. The average resistivity of bornite varies from 5×10^{-3} to 5×10^{-1} of an ohm meter.

Since

$$\sigma = \frac{1}{\rho}$$

where σ = conductivity in mhos per meter

ρ = resistivity in ohm meters

then $\sigma_{\text{Bornite}} = 2 \times 10^2$ to 2 mhos per meter

Thus, the conductivity of bornite varies between 200 mhos per

meter to 2 mhos per meter, depending on the sample location and sample homogeneity.

Considering a model material for bornite,

$$\sigma_m = 1000\sigma_{Bornite}$$

Thus, the material must fall within the range of 2×10^5 to 2×10^3 mhos per meter conductivity in order to simulate bornite.

One material which falls into the scale range of the minerals considered is graphite. Electrode graphite, having a conductivity on the order of 1.223×10^5 mhos per meter was used as the model material. Graphite considerations are given in Appendix A. This satisfied the scale conductivity requirements.

Similarly, by reason of the 1 to 10 scale ratio, a specimen located 1 inch from the tool should represent a sulfide body of a similar geometrical configuration linearly 10X as large located 10 inches from a full sized induction logging tool. Further treatment of these factors is given under section K in Chapter IV and section B in Chapter V.

Minerals & Ores	Resistivity (ohm meters)	Conductivity (mhos per meter)	Scale Conductivity (mhos per meter)
Bornite	5×10^{-3}-5×10^{-1}	2×10^{2} - 2	2×10^{5}- 2×10^{3}
Chalcocite	1×10^{-3}-6×10^{-1}	1×10^{3}- 1.66	1×10^{6}- 1.66×10^{3}
Chalcopyrite	1.5×10^{-4}-3.5×10^{-1}	6.67×10^{2}-2.860	6.67×10^{5}-2.86×10^{3}
Chalcopyrite-Pyrrhotite	1×10^{-3}	1×10^{3}	1×10^{6}
Cobalt-Iron	5×10^{-4}	2×10^{3}	2×10^{6}
Copper	1.5×10^{-8}-1.5×10^{1}	6.67×10^{7}-6.67×10^{-2}	6.67×10^{10}-6.67×10^{1}
Copper-Iron	7×10^{-3}	1.41×10^{2}	1.41×10^{5}
Covellite	1×10^{-3}	1×10^{3}	1×10^{6}
Galena	3×10^{-5}-2×10^{-1}	3.33×10^{4}-5x10	3.33×10^{7}-5×10^{3}
Specular Hematite	4×10^{-3}	2.5×10^{2}	2.5×10^{5}
Magnetite	6×10^{-3}-5×10^{1}	1.66×10^{2}-2×10^{-2}	1.66×10^{5}-2×10^{1}
Molybdenite	1×10^{-3}-5×10^{-1}	1×10^{3}- 2	1×10^{6}-2×10^{3}
Nickel	1×10^{-7}x1.5x10^{-3}	1×10^{7}-6.67×10^{2}	1×10^{10}-6.67×10^{5}
Nickel-Cobalt	5×10^{-4}-6×10^{-3}	2×10^{3}-1.66×10^{2}	2×10^{6}-1.66×10^{5}
Pyrite	1×10^{-6}-5×10^{-4}	1×10^{6}-2×10^{3}	1×10^{9}-2×10^{6}
Pyrite-Chalcopyrite	1×10^{-3}	1×10^{3}	1×10^{6}
Pyrite-Pyrrhotite	1×10^{-3}	1×10^{6}	1×10^{6}
Pyrolusite-Psilomelane	5×10^{-3}	2×10^{2}	2×10^{5}
Pyrrhotite	5×10^{-4}- 5×10^{-2}	2×10^{3}- 2×10^{1}	2×10^{6}- 2×10^{4}

TABLE I

Conductivity Ranges of the Minerals and Ores Simulated in This Investigation (modified after Jakosky, 1960)

IV. EQUIPMENT

A pictorial representation of the equipment utilized, and their physical relationship to each other, is given in Figures 2 and 3. References cited for the circuit diagram, Figure 5, may be compared to the flow diagram in Figure 4 for clarification.

A. Cabinet

All equipment, other than the oscilloscope, vacuum tube volt meter, shielded coupling transformer, battery power supply, logging tools, shielded leads, and graphite models was placed in a 21½" x 17¼" x 66½" steel cabinet as depicted in Figure 2. The cabinet was mounted on casters and provided a unit which could be located anywhere relative to the external equipment. Two 3/8" x 1-1/2" x 61-1/2" aluminum channels were attached midway between the cabinet cooling louvers, on the 17¼" wide panels, parallel to the long dimensions of the cabinet. These served as hangers for twelve 3/8" x 1-1/2" x 20-1/2" channel cross pieces arranged in a ladder-like position. The internal equipment was mounted on separate aluminum chassis as designed to fit on these crosspieces. This afforded the components readily accessible for servicing and maintenance. A removable louvered steel door was utilized as a precautionary shielding measure. Background "fuzz" on the testing oscilloscope disappeared after the cabinet door was installed.

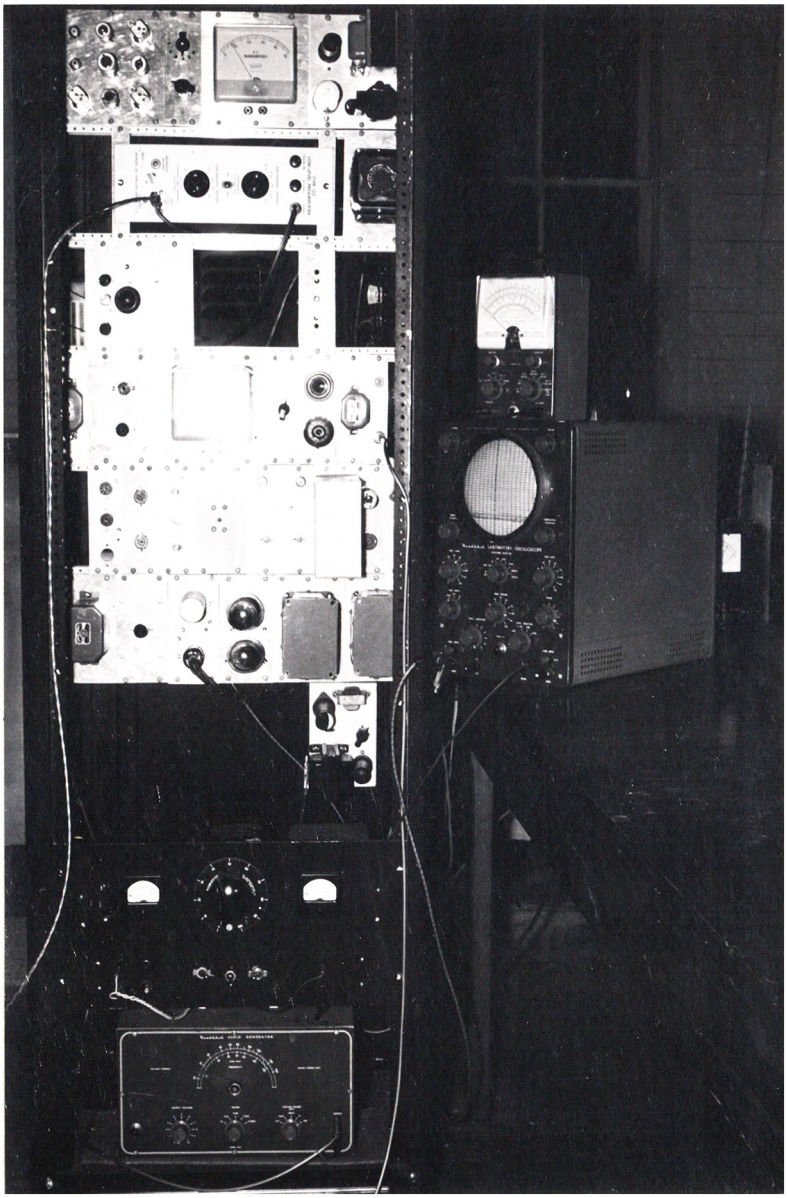

Figure 2. Equipment Setup, Showing Components Mounted in Cabinet

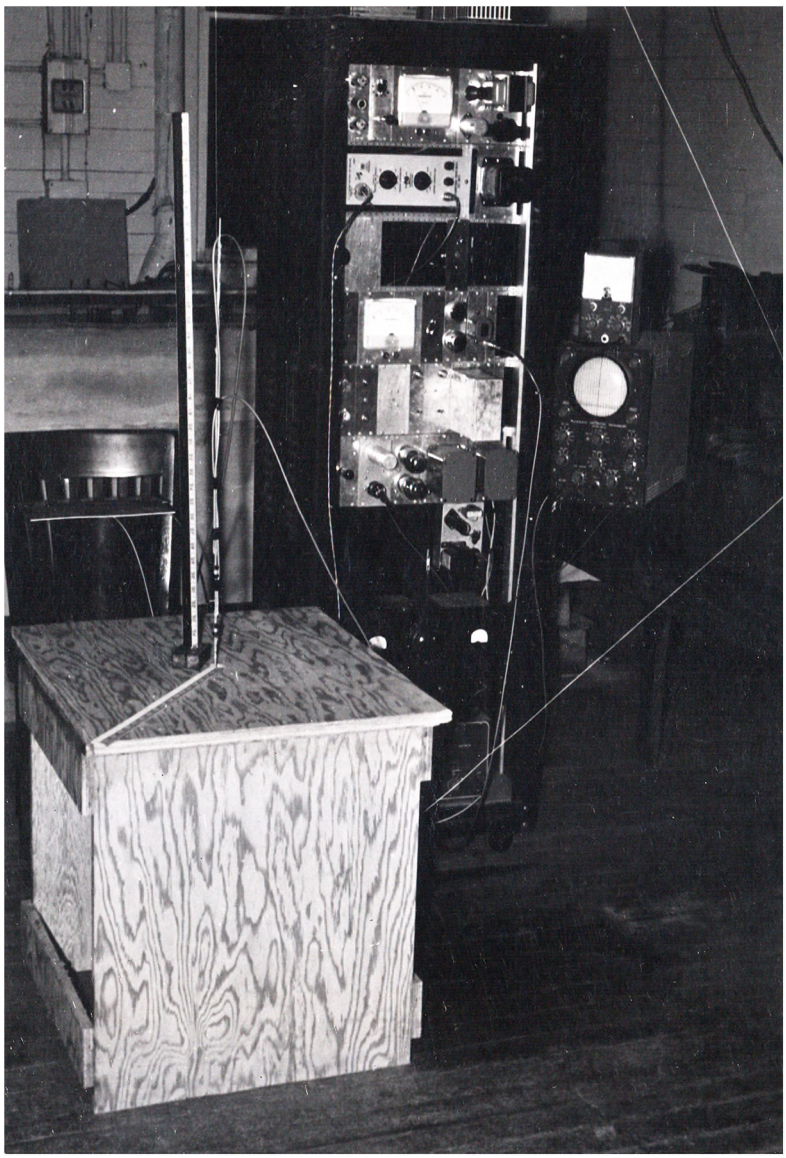

Figure 3. Equipment Setup, Showing Relationship of all Components

B. Signal Generator

The signal generator was a Heathkit audio generator (Model AG-8) capable of 10 volts AC output at a frequency of 2000 cps. It was calibrated by means of Lissajou's figures against another signal generator known to be correct at the 2000 cps range. The unit was oriented at various locations about the cabinet, and effected the other components least when situated at the base. The output of the unit was connected to the power amplifier input via shielded cable. Since this signal generator is available commercially, no circuitry details are given.

C. Power Supply

The power supply provided the B^+ and filament voltages necessary to drive the power amplifier. It consisted primarily of a heavy duty shielded transformer, 5Y3 dual diode, and two-OB2 voltage regulators. Its output was 450 VDC (full-wave rectified) -150 for bias voltage, and 6.3 VAC filament voltage. This was carried to the power amplifier by menas of a twisted bundle cable terminating in an octal connector. In order to minimize the effects of any stray fields associated with the power supply, it was situated at the bottom of the cabinet, approximately two feet below the power amplifier.

D. Power Amplifier

The power amplifier was energized via an octal plug input from the power supply. A signal input of 5.5 VAC at

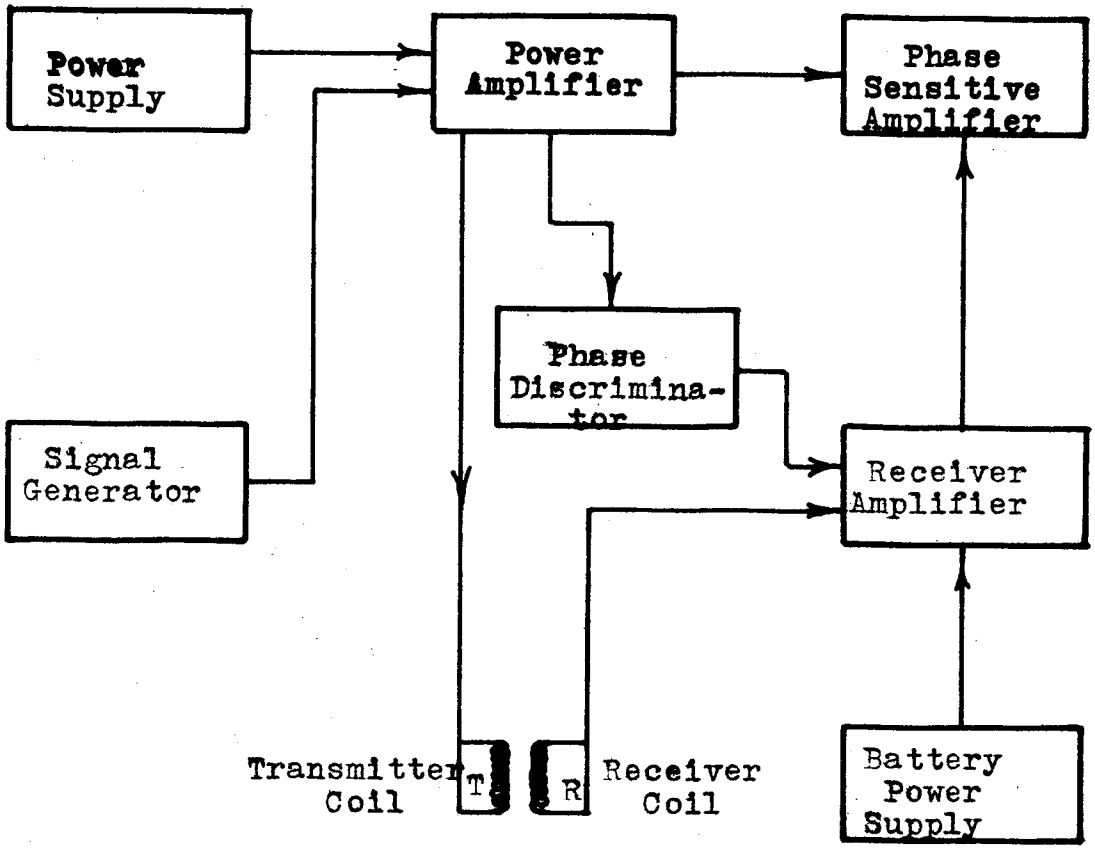

Fig. 4 Flow Diagram of Primary Components

2000 cps from the signal generator was transformer coupled to the grid of the 12BH7 tube. The amplified signal was capacitor coupled to the control grids of the 6550 pentodes and carried from the pentodes to the primaries of two output transformers connected in parallel. The secondary of the first output transformer provided a reference waveform to the phase discriminating network and energized the transmitter coil on the induction tool. Pertinent circuitry details only are depicted in Figure 5. The transmitter coil was maintained at a steady .35 VAC at 2000 cps through a shielded cable. By means of another shielded cable, the output from the secondary of the second output transformer was connected to the phase sensitive amplifier to provide the inphase voltage requisite for the receiver waveform amplification. The entire unit was mounted approximately 6" away from other component units in an effort to minimize stray field effects.

E. Battery Operated Receiver Amplifier

The power amplifier was 135 volts DC positive, and 6.3 volts DC; all from batteries through an octal plug. The batteries were conveniently located on the top of the equipment cabinet. High and low pass filters were provided within the amplifier. The high pass filter with a cut off frequency of 80 cps removed much of the 60 cps noise and the low pass filter with a cut off frequency of 10,000 cps removed much of the high frequency noise. The amplifier input was the

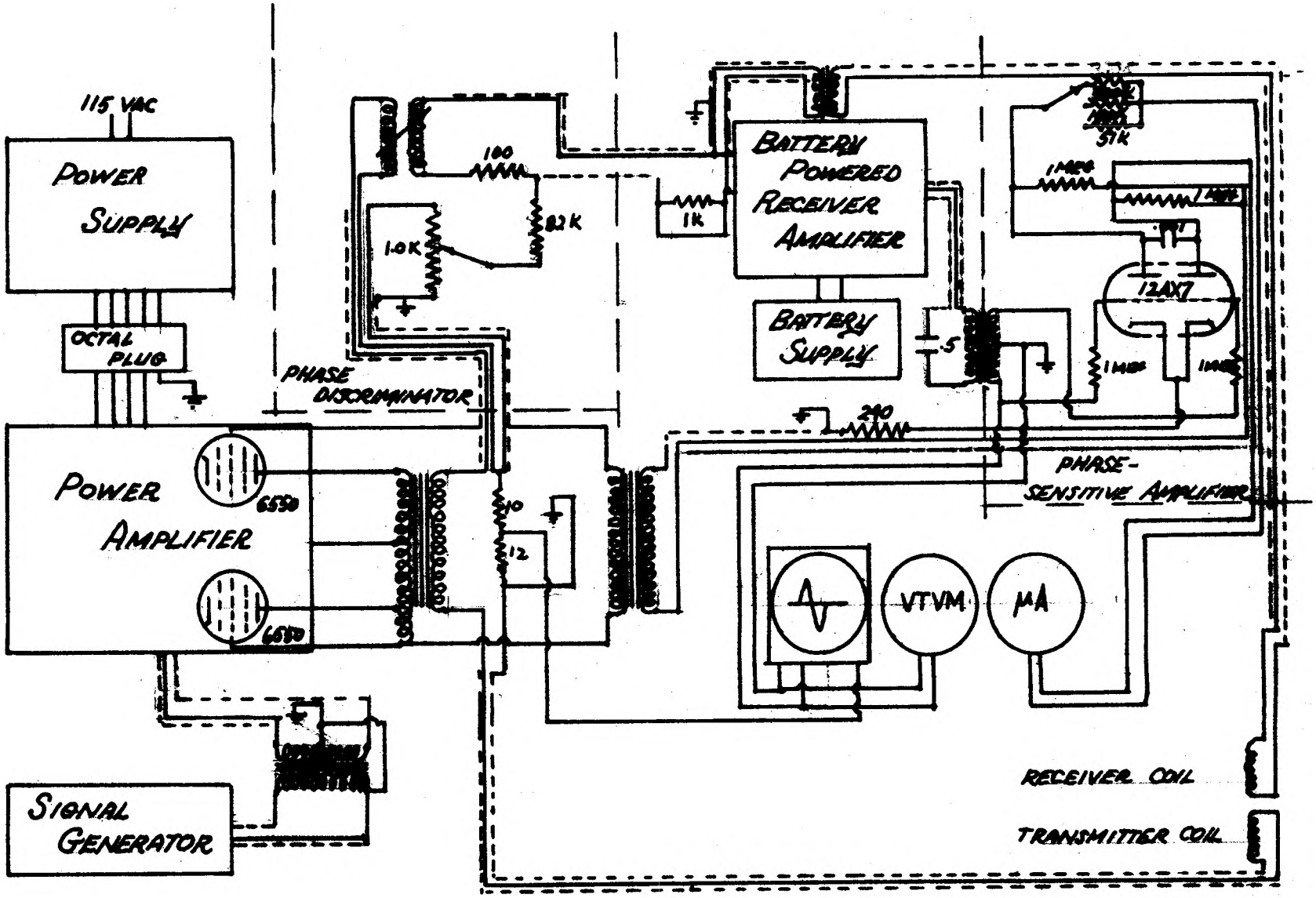

Figure 5. Circuit Schematic. Standard or Component Units Available Commercially are Represented by Blocks.

receiver coil, and output was the phase sensitive amplifier, each connected via shielded cable and transformers.

F. Phase Discriminator

The phase discriminator consisted of two separate 2000 cps signals, one inphase and one 90° out of phase with the transmitter current. The amplitude of these signals was controlled by a linear precision potentiometer (Borg Micropot, Model No. SA154) of 1000 ohms resistance. The circuitry details are given in Figure 5. The two signals were combined and connected to the input of the battery powered receiver amplifier in combination with the signal from the receiver coil. These two signals were used to reduce the output of the battery powered receiver amplifier to zero, when the coil was in air, and away from any conducting body.

It would have been possible to have used the microammeter in the phase sensitive amplifier to indicate a null, then the dial reading of the inphase potentiometer for zero output when near a conducting body would have been a measure of the effect of the conducting body.

G. Phase Sensitive Amplifier

The phase sensitive amplifier consisted primarily of a small coupling transformer, a 12AX7A dual triode, and a wide scale Triplett Model 420-PL microammeter. This relationship is shown in Figure 5. The receiver coil voltage, after being amplified by the battery powered amplifier was transformer coupled to the grids of the 12AX7A dual triode in the phase

sensitive amplifier, and amplified again. Since the plate supply was 2000 cps AC, only the inphase component of the receiver voltage was amplified by the phase sensitive amplifier. The microammeter served as an indicator of the voltages induced in the receiver coil; i.e., a measure of the conductivity in the vicinity of the induction logging tool. Since the microammeter was utilized as a measuring device, it is described further in section H of this chapter. Locationwise, the phase sensitive amplifier was situated on the same level as the phase discriminator, only next to the opposite side of the cabinet.

H. Measuring Devices

Other than the application of Tektronix oscilloscope and Simpson multimeter in the construction of the equipment, the measuring devices consisted of a Heathkit vacuum tube voltmeter (Model V7-A), a Heathkit oscilloscope (Model O-10), and the Triplett microammeter. The voltmeter and oscilloscope gave an indication of the value of the inphase voltage and its actual phase relationship. The microammeter served as a direct measure of the inphase voltage induced in the receiver coil. Hence, once the meter reading and its conductivity relationship was established by calibration, the microammeter served as a "conductivity meter".

I. Tools

The term "tool" refers to the entity consisting of the transmitting and receiving coils and the insulating mandrel

which supported them. The tool shown in Figure 6 consisted of a 0.160 diameter, 15" long wooden mandrel with two coils, spaced 4" apart. Each coil was made from 150 turns of #30 cotton wrapped copper wire and measured .160 of an inch inside diameter, .330 inches outside diameter, and was .350 of an inch long. The coil leads for the tool were tied to shielded cables by pin terminals on the mandrel. Originally, the tool mandrel was machined from a lucite rod, but the heat generated by the coils distorted it and its brittleness rendered it unfit for this investigation.

J. Shielded Cable Leads

Input and output connections and the tool leads were shielded cables. Nearly all of the cable used was Belden single conductor shielded, plastic insulated, microphone cable (Belden #8401-100). All of the leads were as short as practicable with the exception of the tool leads. Generally the tool leads were 8 feet long for tool mobility purposes and were terminated by male or female microphone connectors to facilitate changes. In the few cases where the Belden cables were not adequate for shielding purposes, such as the connections from the power amplifier and battery powered amplifier to the phase discriminator, bi-conductor shielded cables were used. Because of the shielded cables, field effects of units adjacent to the cables were negligible.

K. Models

The model shapes were chosen for the similarity in

Figure 6. Model Induction Logging Tool

geometry (within practical limits) to naturally occurring orebodies. The cylinders represented chimneys, pipes and portions of massive deposits; the rectangular prism and parallelpipes represented prismlike orebodies and veins, pods, sills, displaced beds, and rectangular portions of massive deposits; and the slabs represented veins, sills, dikes, and thin displaced portions of beds. The shapes are illustrated in Figure 7. Graphite was chosen as a model material because it was readily detectable by the induction logging tools and its conductivity represented that of a wide range of conductive ore minerals. Materials possessing electrical properties suitable for scale model studies were difficult to obtain, even more difficult to fabricate, so the study was restricted to the minerals outlined in Table I.

L. Testing Tables

A 24 inch high testing table served as a support for the models during the actual investigations. Figure 3 and Figure 9 show its relationship to the equipment and its usage. It was constructed of 3/4 inch thick, five ply plywood. Glued joints were used in its construction, hence the table was non-conductive. A 1-1/4 inch hole was bored through the center of the table top. This permitted the induction tool to be passed below the model under study. Logging "trips" through the hole without a model on the table top showed no conductivity effects.

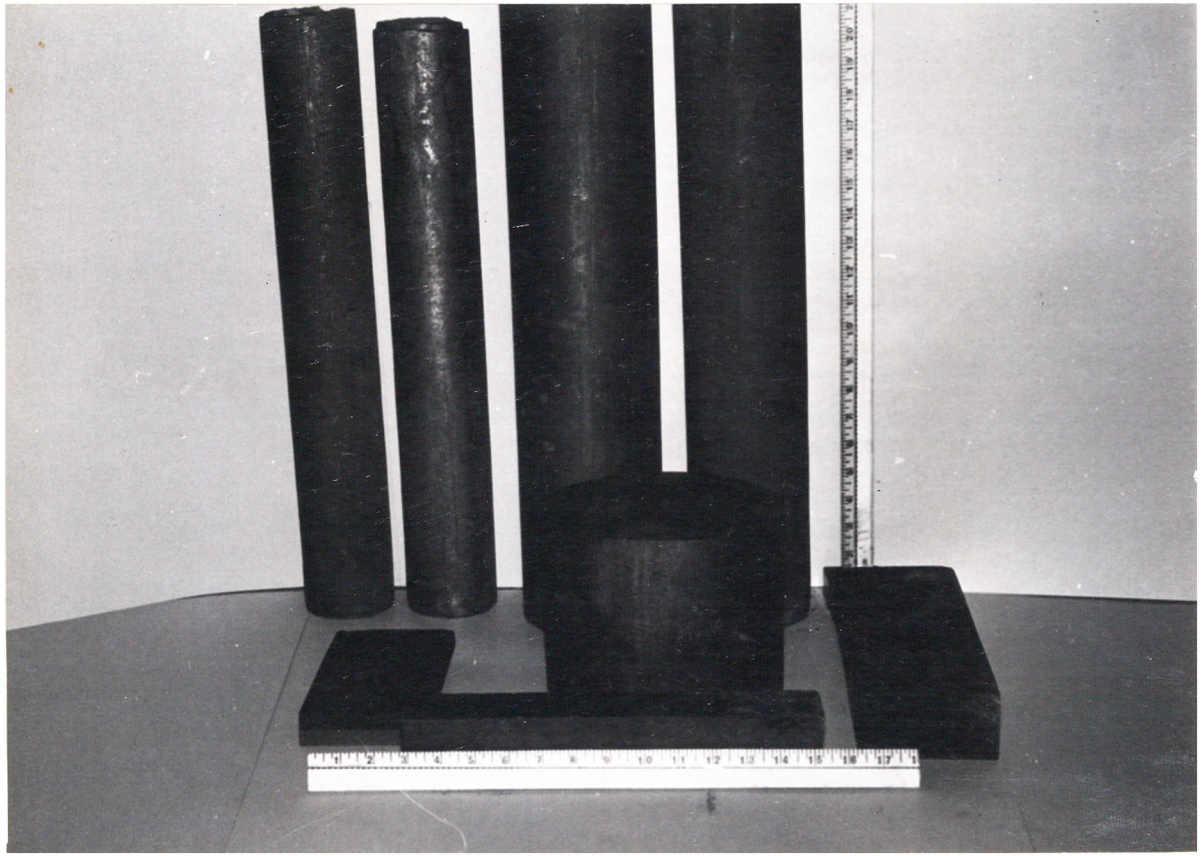

Figure 7. Graphite Models Used to Simulate Sulphide Orebodies.

V. PROCEDURES

A. Equipment Calibration

When the variable tuning coil and the precision potentiometer in the phase discriminator were adjusted properly, the voltmeter read nearly zero if the induction logging tool was in air. This meant that the currents induced by mutual induction between the transmitter and receiver were rendered negligible by the discriminator, and that a practical zero or null had been achieved. The microammeter on the output of the phase sensitive amplifier was adjusted to serve as an indicator of the inphase component of the receiver coil voltage. It's "zero" was set so that the meter could deflect to either side. This deflection was proportional to the quadrature component of the current induced in the body which depended on the conductivity and geometrical shape of the body.

B. Tool Calibration

A saturated sodium chloride solution, having a conductivity of 29 mhos per meter at a temperature of 89°F. was placed in a five gallon jug. A glass tube "borehole" of 5/8" inside diameter was then placed in the brine, which was effectively an infinite medium. The dimensions of the jug permitted approximately 95% of the geometrical factor to be included within its confines. Doll's (1949, p. 6) geometrical factor chart gives this relationship. Doll (1949, p. 3) and Duesterhoeft (1961, p. 193) consider borehole effects negligible except for extreme cases. The data used for the brine calculation is given in Appendix B.

When the tool was immersed in the brine via the "borehole" a scale deflection was noted on the conductivity meter at a .303 x multiplier setting and on the 1x multiplier setting. Therefore, since the 1x multiplier was used throughout the model runs, the calibration for the multiplier was 116 mhos per meter per scale division. This calculation is given in Appendix C.

According to Duesterhoeft (1961, p. 194), the voltage in the receiver of a two coil induction log located in a homogeneous medium is approximated by the following relationship:

$$V_r = \frac{j\omega\mu A_t A_r I_t}{2\pi L^3}\left\{1 - (j\omega\mu\sigma)L^2/2 + (j\omega\mu\sigma)^{3/2}L^3/3 - (\omega\mu\sigma)^2 L^4/8 + (j\omega\mu\sigma)^{5/2}\frac{L^5}{30} \cdots\right\}$$ Duesterhoeft Equation 10

where

V_r = voltage induced in the receiver coil

ω = 2 x frequency

μ = permeability (the permittivity of free space is customarily used)

A_t = coil area of the transmitter

A_r = coil area of the receiver

I_t = current in the transmitter

L = coil spacing

σ = the conductivity of the medium

Duesterhoeft (1961, p. 194) states that . . ." the first term is the voltage due to the mutual induction of the coils, the second term is proportional to the conductivity of the medium, and the remaining terms take into account propagation or

skin effect". This equation is in agreement with the results of Zenor and Oshry (1962), and can be represented by:

$$V = V_m + V_\sigma + V_s$$

where

V_m = voltage due to mutual inductance

V_σ = voltage due to conductivity without skin effect

V_s = voltage correction due to skin effect

Since for a non-magnetic medium, μ is considered as the permittivity of free space, then for any given tool, the voltage due to mutual inductance is invariant provided that the variables such as frequency and transmitter current remain unchanged. Therefore, V_m, or the voltage due to mutual inductance, will be a constant for a given tool.

For the case where skin effect is negligible, the voltage component V_σ due to conductivity is given by:

$$V = V_m (\omega\mu\sigma) \frac{L^2}{2} \quad \text{.....(From Duesterhoeft's Equation 10)}$$

where the terms have the same meaning as described earlier. Again, for any given tool, everything will remain constant in a non-magnetic medium except for the conductivity σ. Therefore,

$$V_\sigma = K\sigma$$

where

K = constant of proportionality $(V_m \omega\mu) \frac{L^2}{2}$.

Since the current through the microammeter or (conductivity meter) is directly proportional to the voltage induced in the receiver coil, it is an indicator of conductivity.

The only variable, then, is the conductivity of the medium, and a linear relationship is established.

The voltage component V_s, due to skin effect, becomes appreciable only when the conductivity of the medium is high. Skin effect is negligible when frequencies in the order of 2000 cps and conductivities of the order of brine solutions are utilized. Since skin effect has been calculated assuming symmetry of revolution, its application to asymmetrically located bodies are difficult to calculate.

A calibration curve based on voltage proportionally, is given for apparent conductivity vs. scale deflection in Figure 8. Apparent conductivity is used because it is the custom of the industry.

C. Model Runs

The tool was suspended as shown in Figure 9, perpendicular to the model table, by means of a line whose free ends were attached at both ends of the tool. The line was passed through a floor and an overhead plastic sheave in order to permit bi-directional vertical movement of the tool. Each specimen was"logged" with its long dimension parallel, then perpendicular or askew to the axis of the tool. Initially, each model was placed directly adjacent to the tool, then moved away in half inch increments on a radius in the plane of the table top. A run was completed on the model before each lateral increment of movement was effected. The maximum radius of investigation, or that point where the influence of each graphite model was no longer detectable, was considered

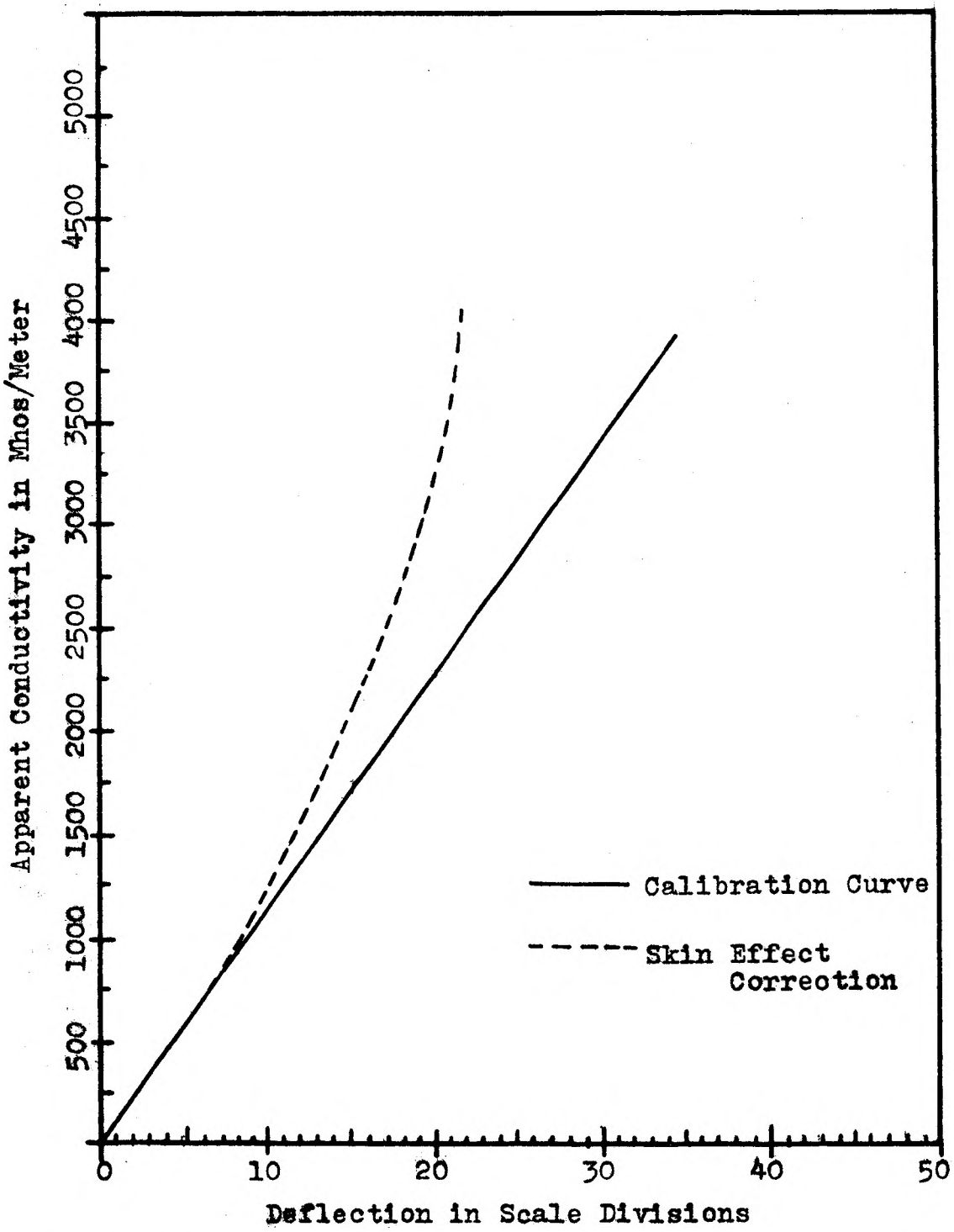

Figure 8. Model Calibration Curve Showing Apparent Conductivity vs. Scale Deflection. Modification Due to Skin Effect is Also Shown. (After Zenor & Oshry, 1962)

as the terminal point of the lateral investigation. Each run commenced two inches above that point in which an initial deflection of the microammeter was noted. Gradational readings were obtained in this manner. The tool was passed downward and stopped in $\frac{1}{2}$" increments. At each stopping point, a reading was taken. This procedure eliminated the effects of lateral oscillation of the suspended tool during the runs. Each specimen was "logged" three times for each lateral location. Runs which differed by a quarter scale division or more were discarded, and the three "acceptable" runs averaged. Only one run was discarded, hence consistency within the accuracy of the meter scale divisions was attained. The results of the runs were reduced to values of apparent conductivity, and graphically represented as curves.

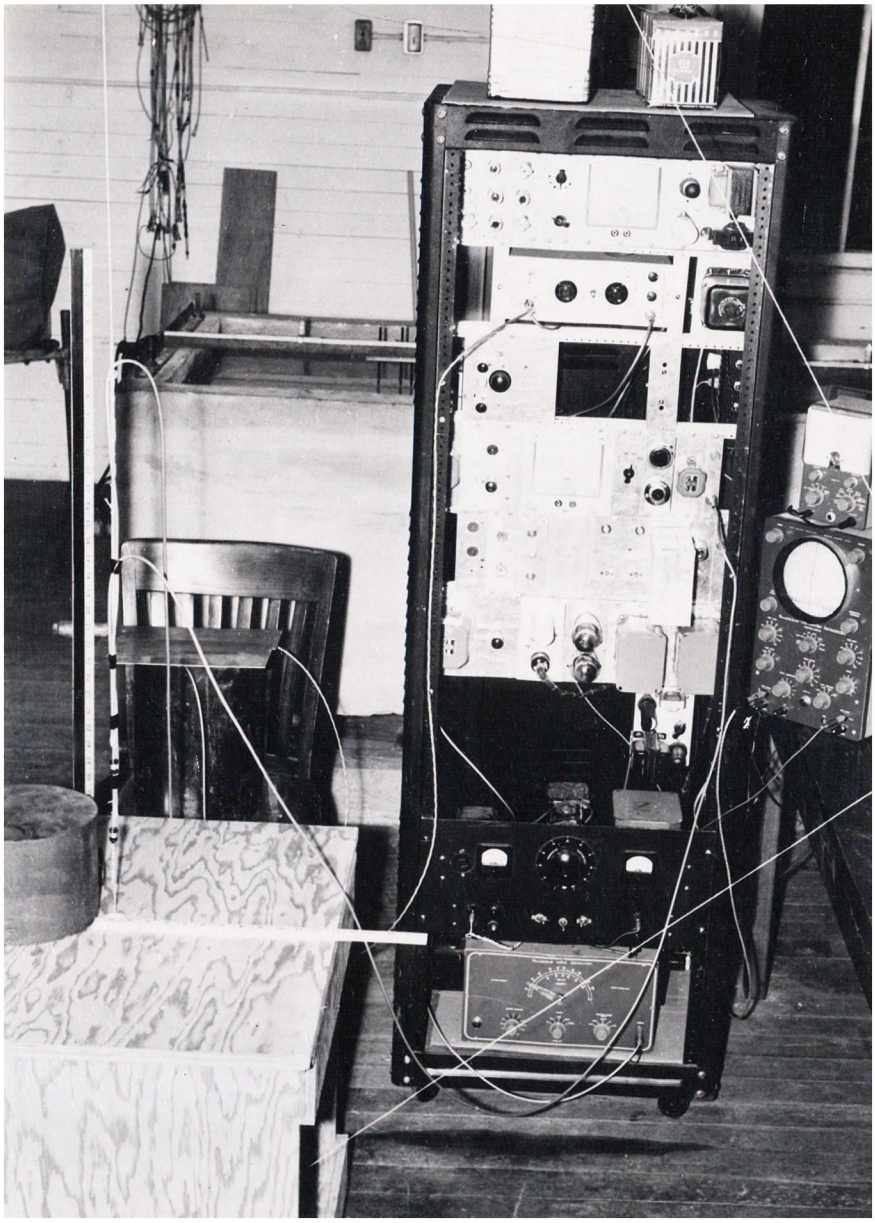

Figure 9. Pictorial Representation of the Logging Method

VI. CONDUCTIVE BODIES IN AIR

In this section, "tool from specimen distance" means the distance in inches that the tool axis was located with respect to the nearest surface of the specimen logged. The point at which the specimen was no longer detectable is termed as the maximum radius of investigation or MRI. The curves were plotted in terms of apparent conductivity since the tool measured the apparent total conductivity of the media it traversed.

For orientation purposes, the longitudinal axis is either the axis of revolution (in cases of the cylinders) or the longest dimension of the specimen (in cases of the prisms).

None of the curves presented are corrected for skin effect. The behavior of skin effect in an asymmetrical case is unknown.

All data obtained in the investigation are presented in a manner consistent with current (1962) induction logging practices. The same graphic scale is used for all curves in order to offer a means of visual comparison.

A. Cylinder (7-3/4" Diameter)

The 6-1/8" long x 7-3/4" diameter cylinder was logged three ways; the tool parallel to the longitudinal axis, perpendicular to the longitudinal axis, and end-on to the longitudinal axis. Figure 10 shows the curves obtained for various tool to specimen distances for a series of runs parallel to the longitudinal axis. It can be seen that a symmetrical relationship is established about a line approximately

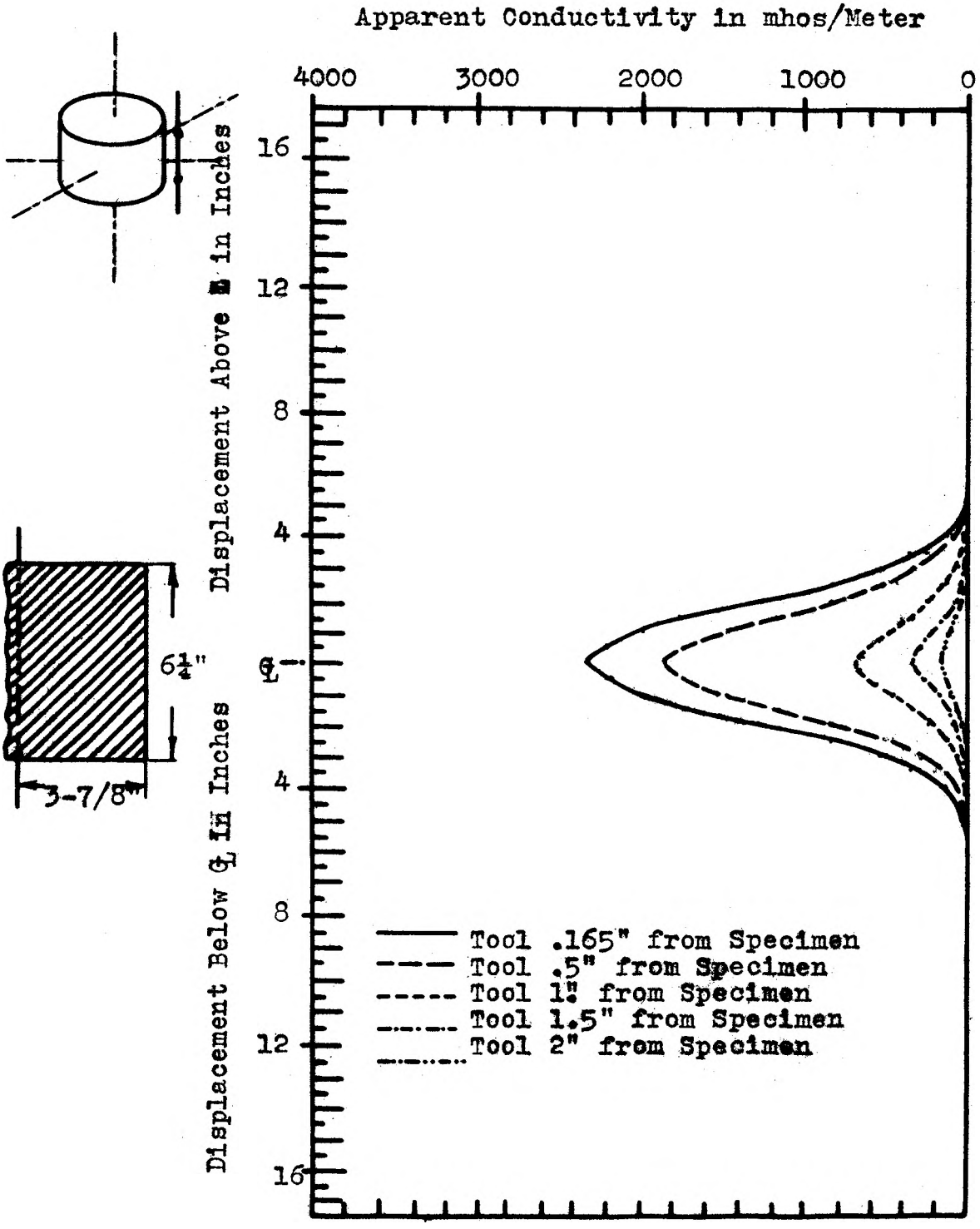

Figure 10. Apparent Cenductivity Curves for a 6-1/8" long x 7-3/4" Diameter Graphite Cylinder in Air. Tool Parallel to Longitudinal Axis. Curves uncorrected for Skin Effect.

through the center of the specimen, and that the broadening of the curve peak is an indication of the body width.

As will be seen in the following pages, the areal geometry of the specimen appears to be related to the maximum value and shape of the curve. Similarly, the peak value decreases with an increase of tool to specimen distances. For this series of runs, at a distance of 3-5/8", the influence of the cylinder is undetectable.

The curves for runs perpendicular to the longitudinal axis are given in Figure 11. When compared to Figure 10, the curves appear symmetrical, but are less broad at their bases. Again, the influence of the body decreases as distance increases. At 3-5/8", the body is no longer detectable. The reader should note that the diameter of the cylinder is greater than the coil spacing of the tool. This will appear as a curve influencing factor when the curves from smaller diameter cylinders are examined.

The figure 12 gives the curve relationship for a series of runs made end-on to the longitudinal axis. The flat surface opposite the tool appears to have a definite shaping influence to the curves. The maximum radius of investigation is 3-3/8" for this orientation.

The "dishing" effect or concave peak should be noted, as it represents a major change in curve shapes thus far. It will be shown in the following pages that a "dished" or concave peak is characteristic of flat surfaces opposite the logging tool. Symmetry is still apparent.

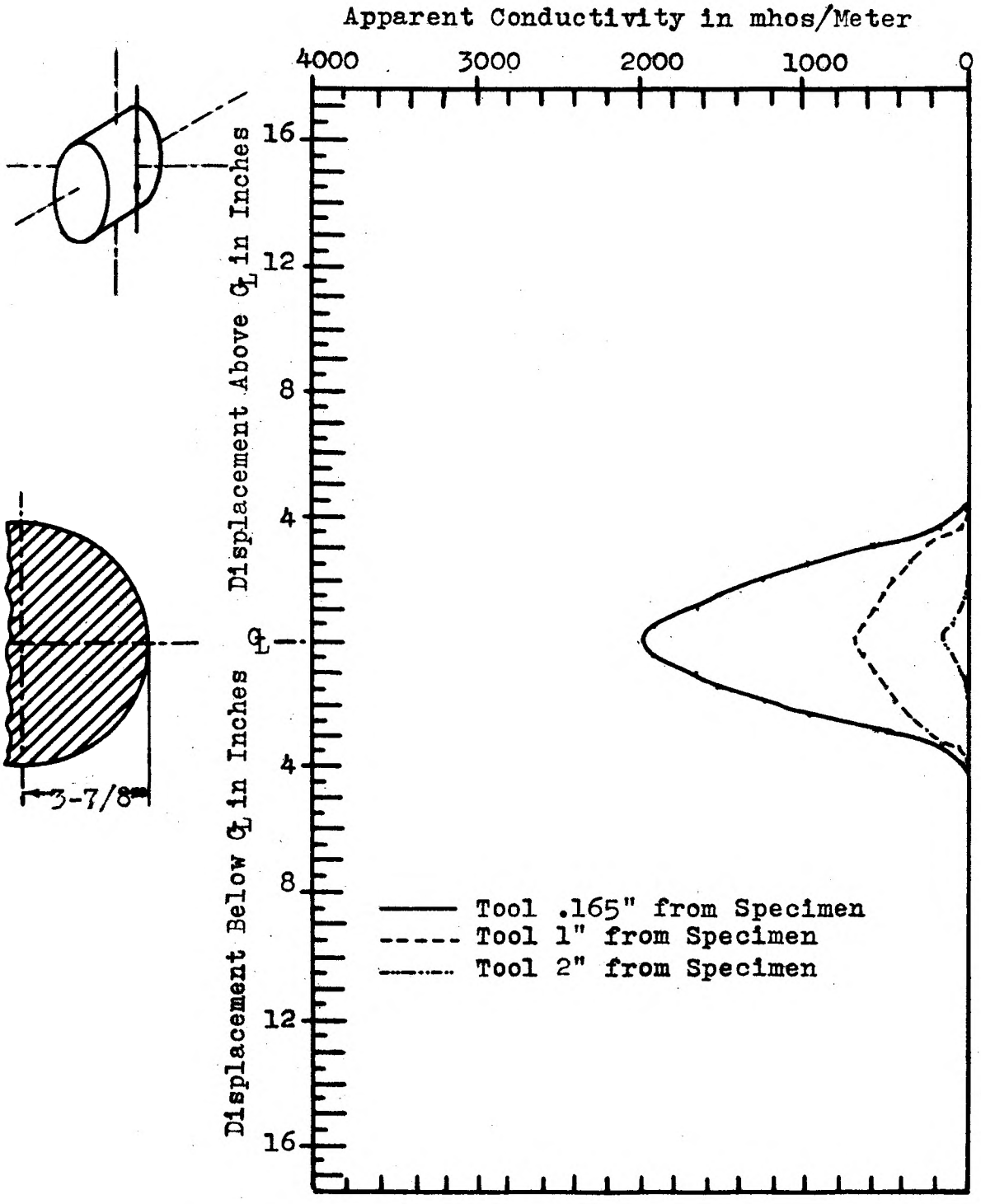

Figure 11. Apparent Conductivity Curves for a 6-1/8" Long x 7-3/4" Diameter Graphite Cylinder in Air. Tool Perpendicular to Longitudinal Axis. Curves Uncorrected for Skin Effect.

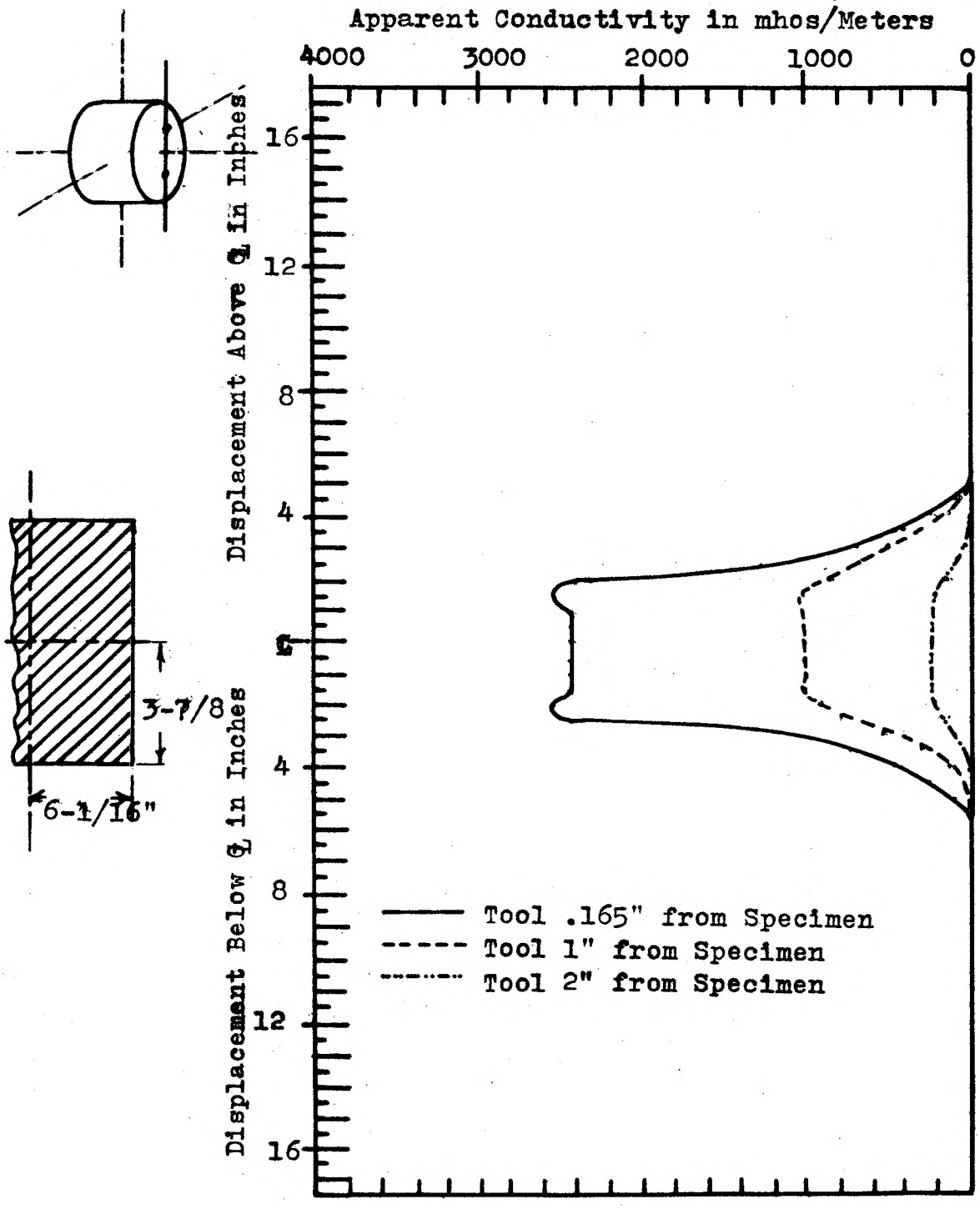

Figure 12. Apparent Conductivity for a 6-1/8" Long x 7-3/4" Diameter Graphite Cylinder in Air. Tool End-on to Longitudinal Axis. Curves Uncorrected for Skin Effect.

B. Cylinder (5" Diameter)

The 30-3/8" Long x 5" Diameter cylinder was logged parallel, perpendicular, and skewed 45° to its longitudinal axis. The parallel runs are depicted in Figure 13. The curves rise to a maximum value, remain constant, then decrease as the end of the body approached. A symmetrical consideration is apparent. The peaks are flat; seemingly due to the homogeneity and consistent dimensions of the cylinder. A maximum radius of investigation of 3" was obtained for this orientation. It should be noted that the top and bottom of the cylinder can be approximated by the inflection points near the base of the curves. This, and the regular, flat peak will be found to be characteristic of cylinders logged parallel to their long dimension.

The curves obtained by logging this cylinder perpendicular with respect to the longitudinal axis are represented in Figure 14. The peaks of the curves are concave only within a 3/4" tool to specimen distance. Beyond that, they take on the characteristic of curves logged traversely to the cylinder axis. As in the past curves, symmetry, about a line passing through the cylinder center, is apparent. The maximum radius of investigation, in this case, is 2-3/4".

The curves for a skewed cylinder are shown in Figure 15. They are no longer symmetrical, but have a bulge effect on their upper portions. The curves appear to be a compromise between the two former series. This compromise may have a relationship to the dip, or angle between the longitudinal axis and a horizontal plane, of the body.

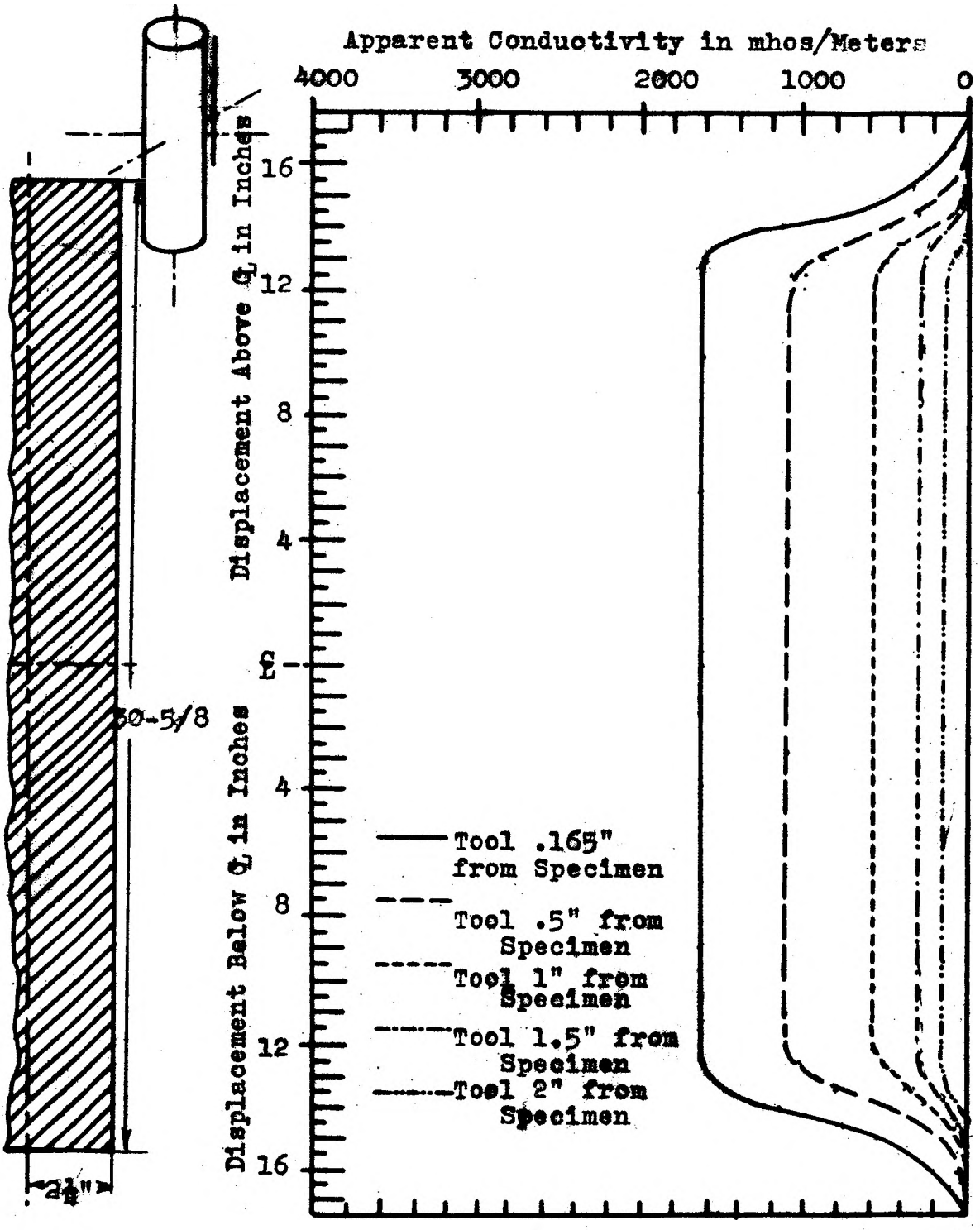

Figure 13. Apparent Conductivity Curves for a 30-5/8" Long x 5" Diameter Cylinder in Air. Tool Parallel to Longitudinal Axis. Curves Uncorreeted for Skin Effect.

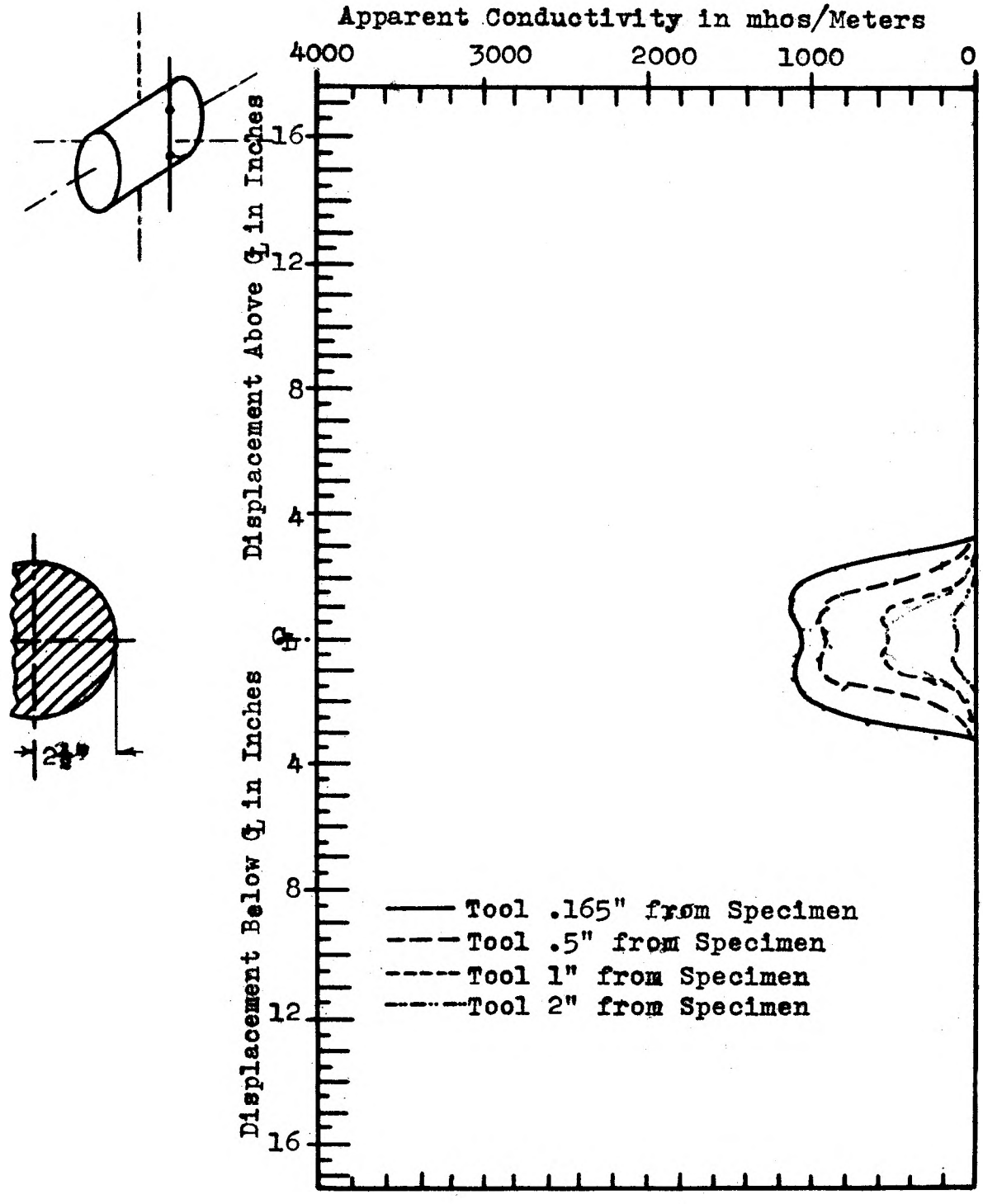

Figure 14. Apparent Conductivity Curves for a 30-3/8" Long x 5" Diameter Graphite Cylinder in Air. Tool Perpendicular to Longitudinal Axis. Curves Uncorrected for Skin Effect.

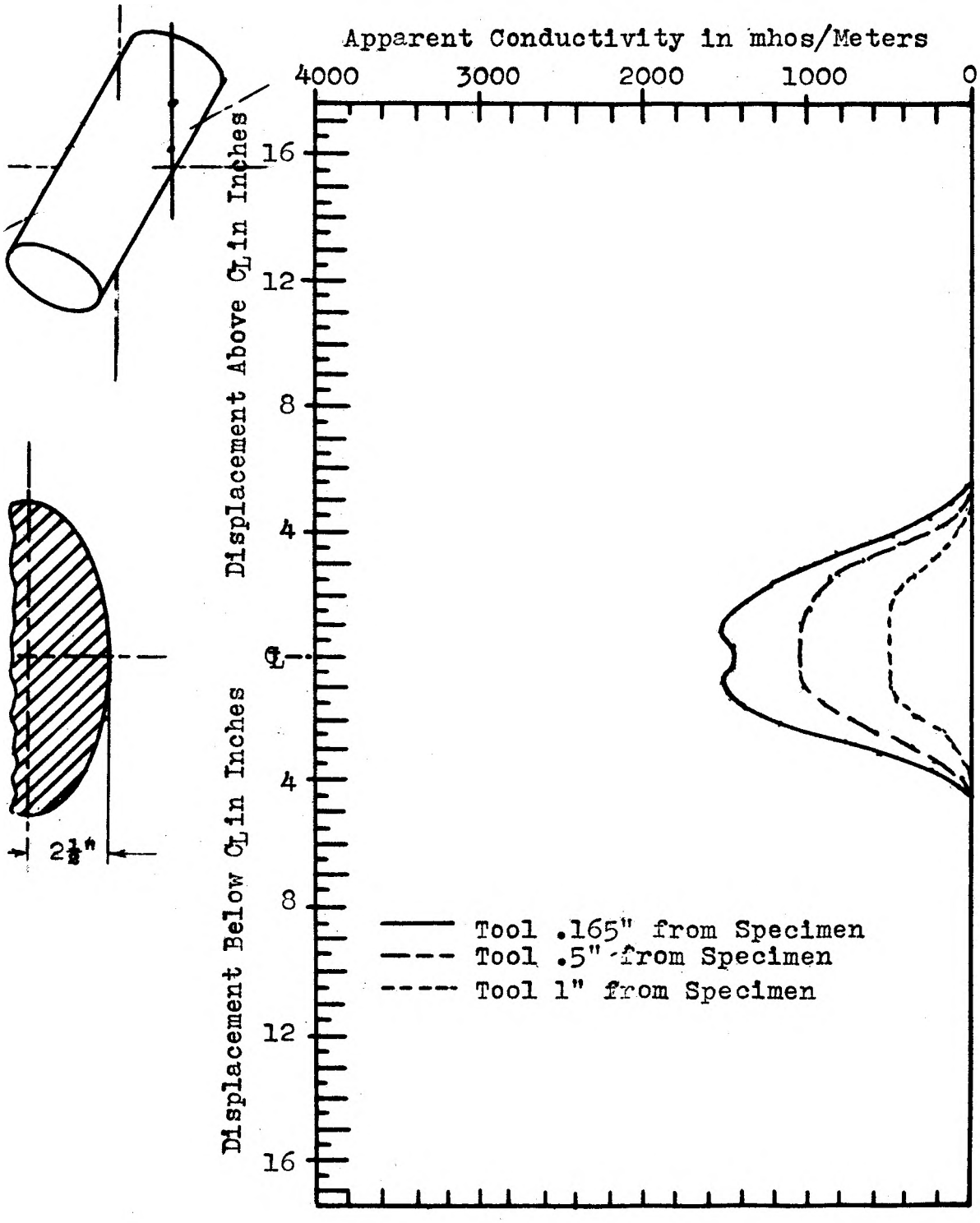

Figure 15. Apparent Conductivity Curves for a 30-3/8" Long x 5" Diameter Graphite Cylinder in Air. Tool 45° to Longitudinal Axis. Curves Uncorrected for Skin Effect.

C. Cylinder (4¼" Diameter)

The 24-5/8" long x 4-1/4" diameter cylinder was logged only parallel to its longitudinal axis. Runs perpendicular to the axis are discussed under faulted bodies in section H of this chapter. The parallel run curves are shown in Figure 16. Examination of these curves shows a remarkable similarity to the curves obtained from the 5" diameter cylinder (Figure 13). As pointed out previously, the ends of the cylinder can be approximated by the inflection points of the curves. A maximum radius of investigation of 2-1/4" was obtained.

D. Cylinder (3¼" Diameter)

The 21" long x 3¼" diameter cylinder was logged parallel to its longitudinal axis. Investigations perpendicular to the axis are discussed under section H of this chapter. From Figure 17, it appears that the usage of inflection points on the curves again approximates the cylinder ends. The peaks of the curves are flat, as expected from previous analysis, and the radius of investigation decreased to 2¼".

E. Orthorhombic Prism (2" x 4" x 12")

The orthorhombic prism was logged parallel to the 4" x 12" face, along the longitudinal axis parallel to the 2" x 12" face, perpendicular to the longitudinal axis; and parallel to the 2" x 12" face, parallel to the longitudinal axis. In the first case, the curves in Figure 18 show a definite relationship between a flat surface and its influence

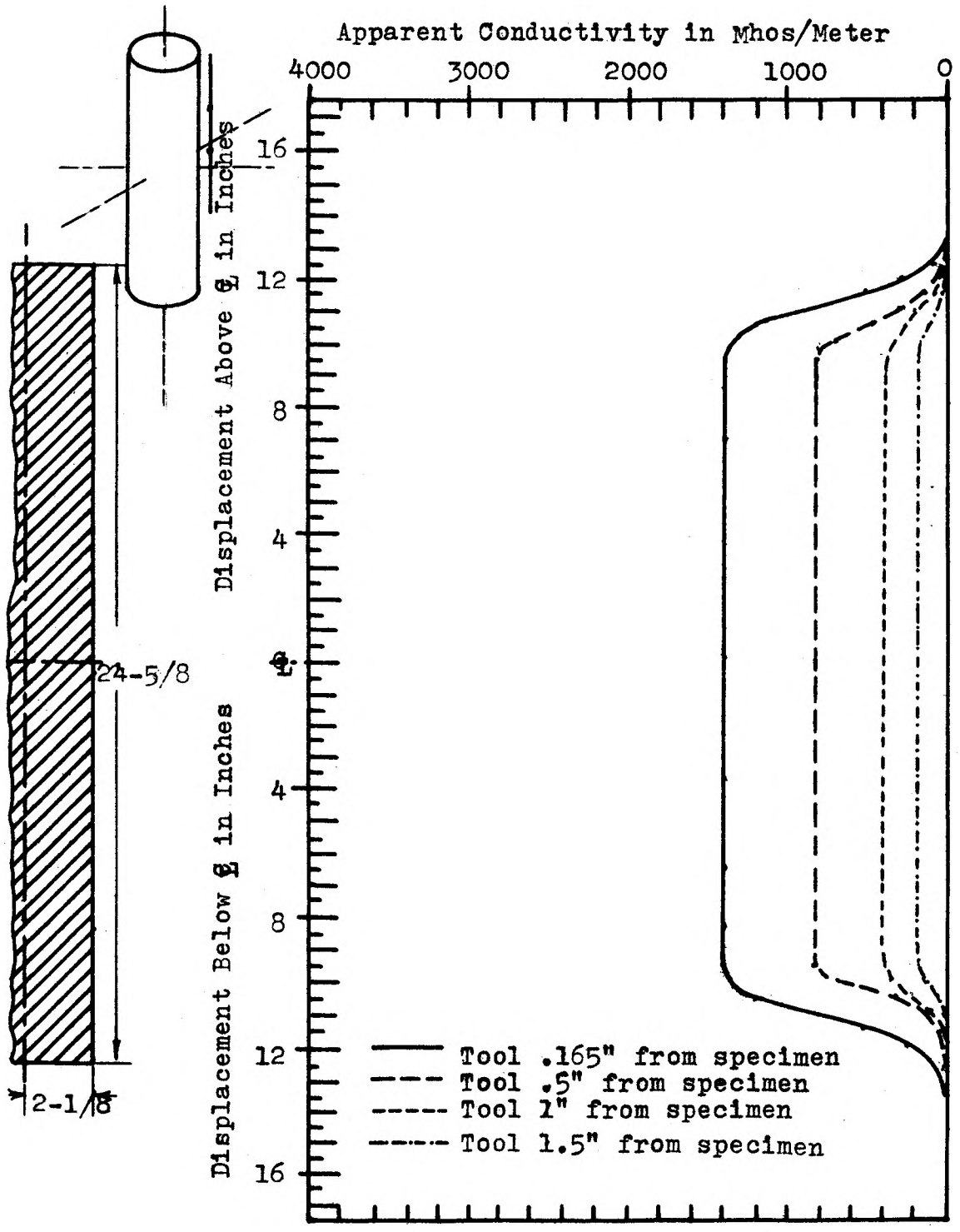

Figure 16. Apparent Conductivity Curves for 24-5/8" Long x 4-1/4" Diameter Graphite Cylinder in Air. Tool Parallel to Longitudinal Axis. Curves Uncorrected for Skin Effect.

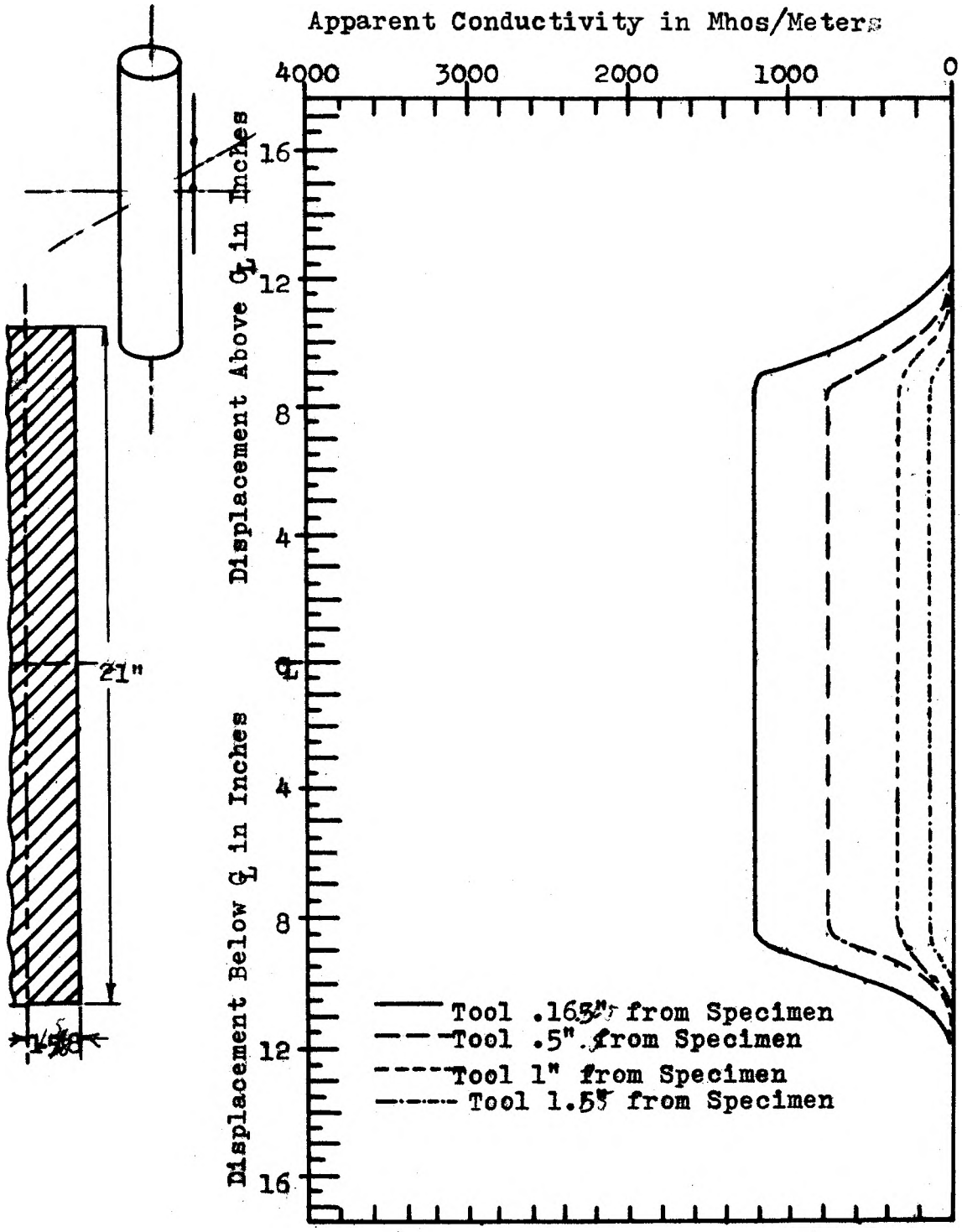

Figure 17. Apparent Conductivity Curves for a 21" Long x 3½" Diameter Graphite Cylinder in Air. Tool Parallel to Longitudinal Axis Curves Uncorrected for Skin Effect.

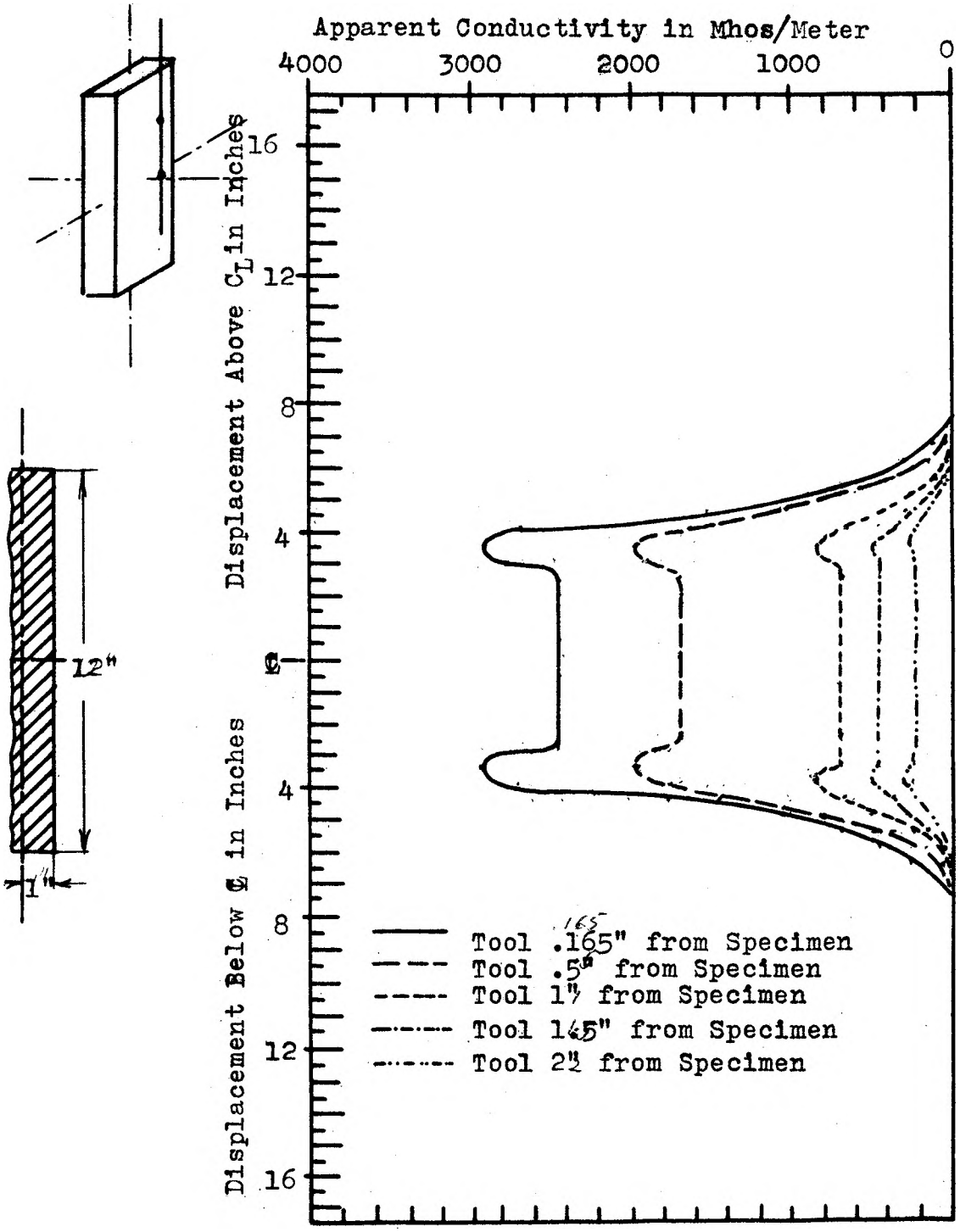

Figure 18. Apparent Conductivity Curves for a 2" x 4" x 12" Graphite Orthorhombic Prism in Air. Tool Parallel to Longitudinal Dimension Along 4" x 12" Face. Curves Uncorrected for Skin Effect.

on the tool. The concave peaks actually appear to resolve into two separate projections which are maintained until the maximum radius of investigation of 3½" is reached. The distance between the peak projections appear to be approximately 2/3 the length of the prism. As will be noted in the succeeding discussion, the prism must have a dimension greater than the tool coil spacing for this analysis to remain consistent.

The curves for a perpendicular traverse are depicted in Figure 19. The peak values are greatly decreased, although the characteristic shape appears to remain consistent for the flat surface relationship. As noted in the previous discussion, the projection on the curve peaks appear to lie outside the edges of the prism. In this case, it appears that the coil spacing, being larger than that of the flat surface, appears to have influenced the curves. The radius of investigation for this case is 1-3/4".

The curves for runs parallel to the longitudinal axis of the 2" x 4" face are shown in Figure 20. The symmetrical peaks have the characteristic shape which seems to be common to flat faced specimens. Analysis of the curve projection peaks appears to bear out the 2/3 relationship of specimen length pointed out previously. The decreased surface area of the specimen seems to have a control on the maximum peak values, when compared to the runs paralleling the 4" x 12" face. The values have decreased, as has the maximum radius of investigation value of 1-5/8".

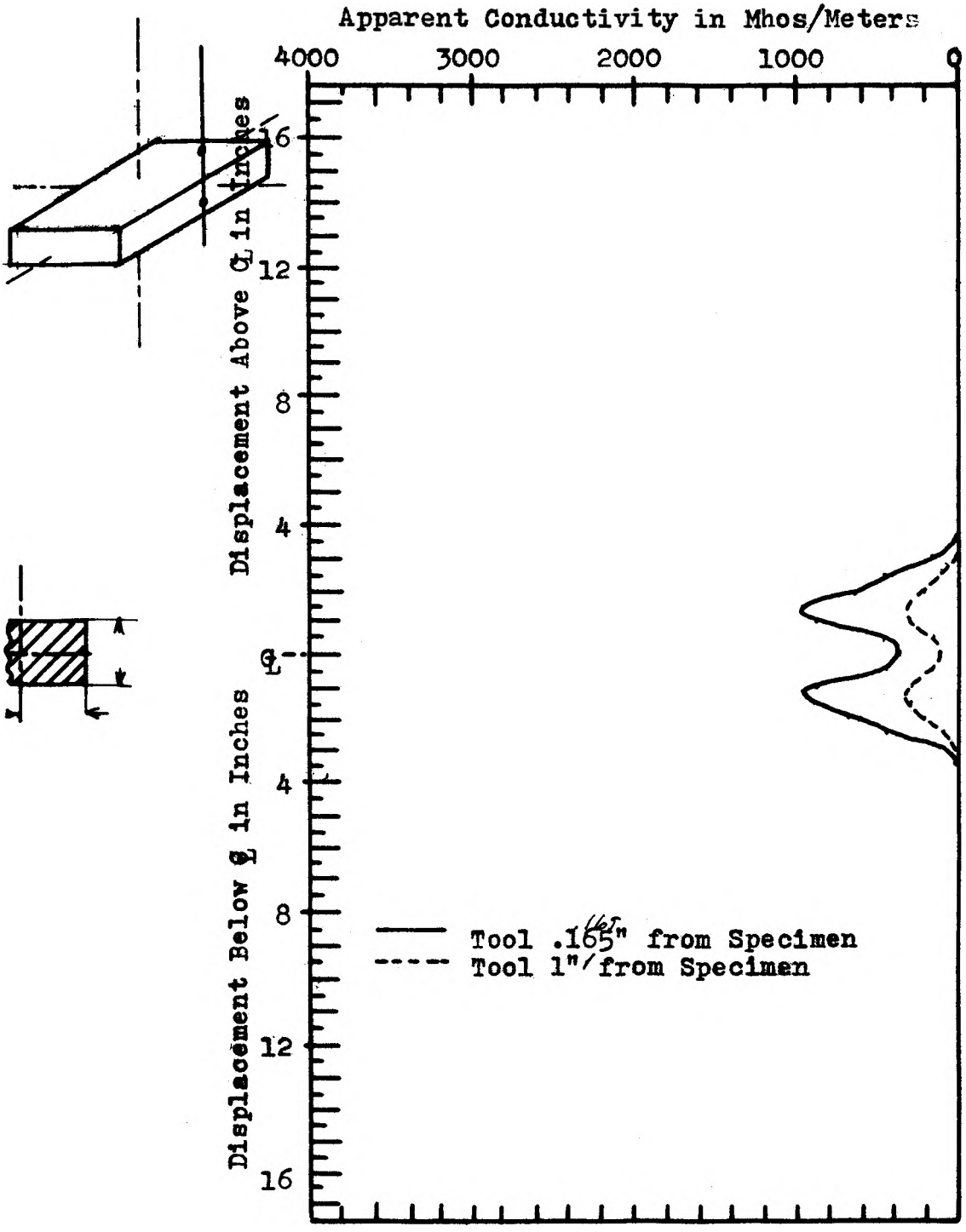

Figure 19. Apparent Conductivity Curves for a 2" x 4" x 12" Graphite Orthorhombic Prism in Air. Tool Perpendicular to Longitudinal Dimension of 2" x 12" face. Curves Uncorrected for Skin Effect.

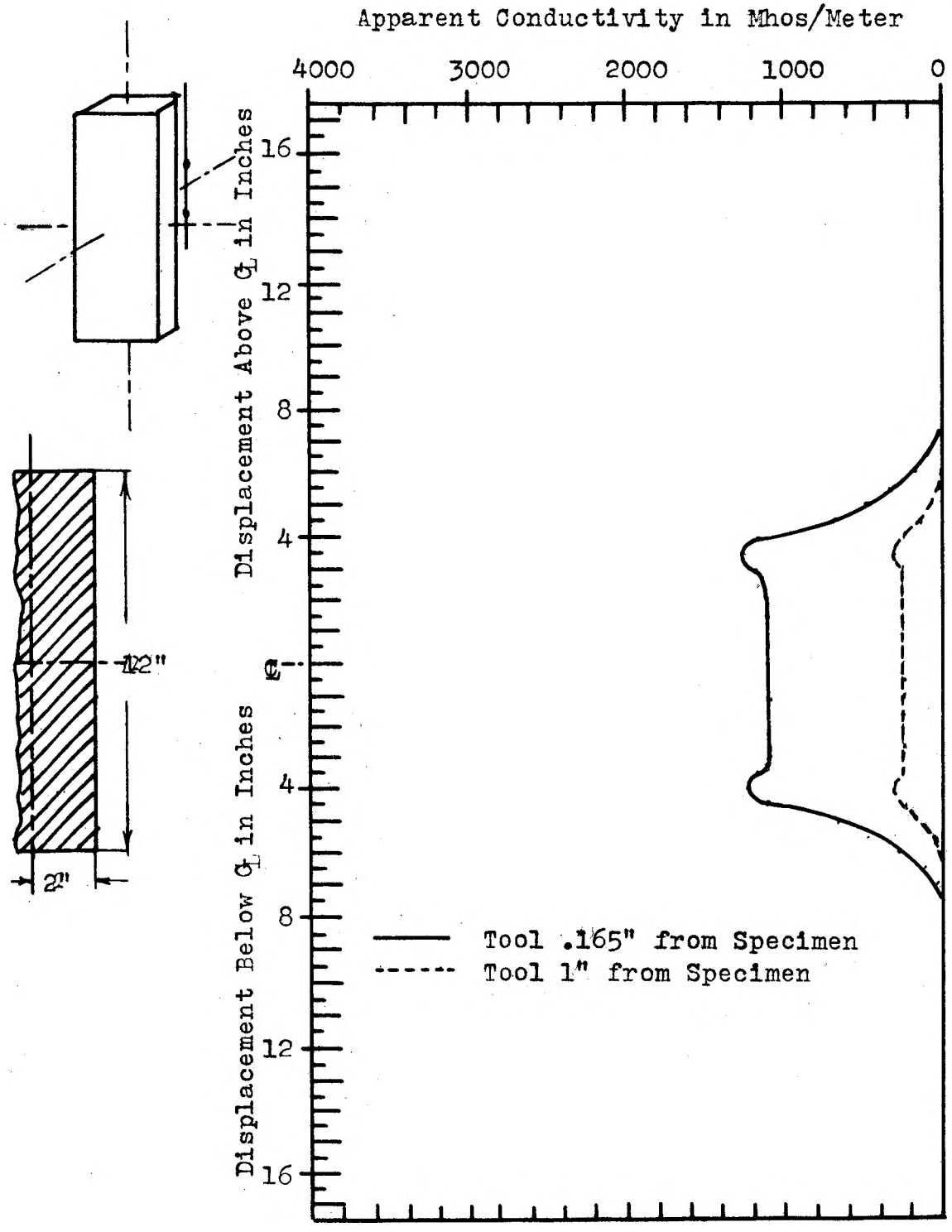

Figure 20. Apparent Coneuctivity Curves for a 2" x 4" x 12" Graphite Orthorhombic Prism in Air. Tool Parallel to Longitudinal Dimension of 2" x 12" Face. Curves Uncorrected for Skin Effect.

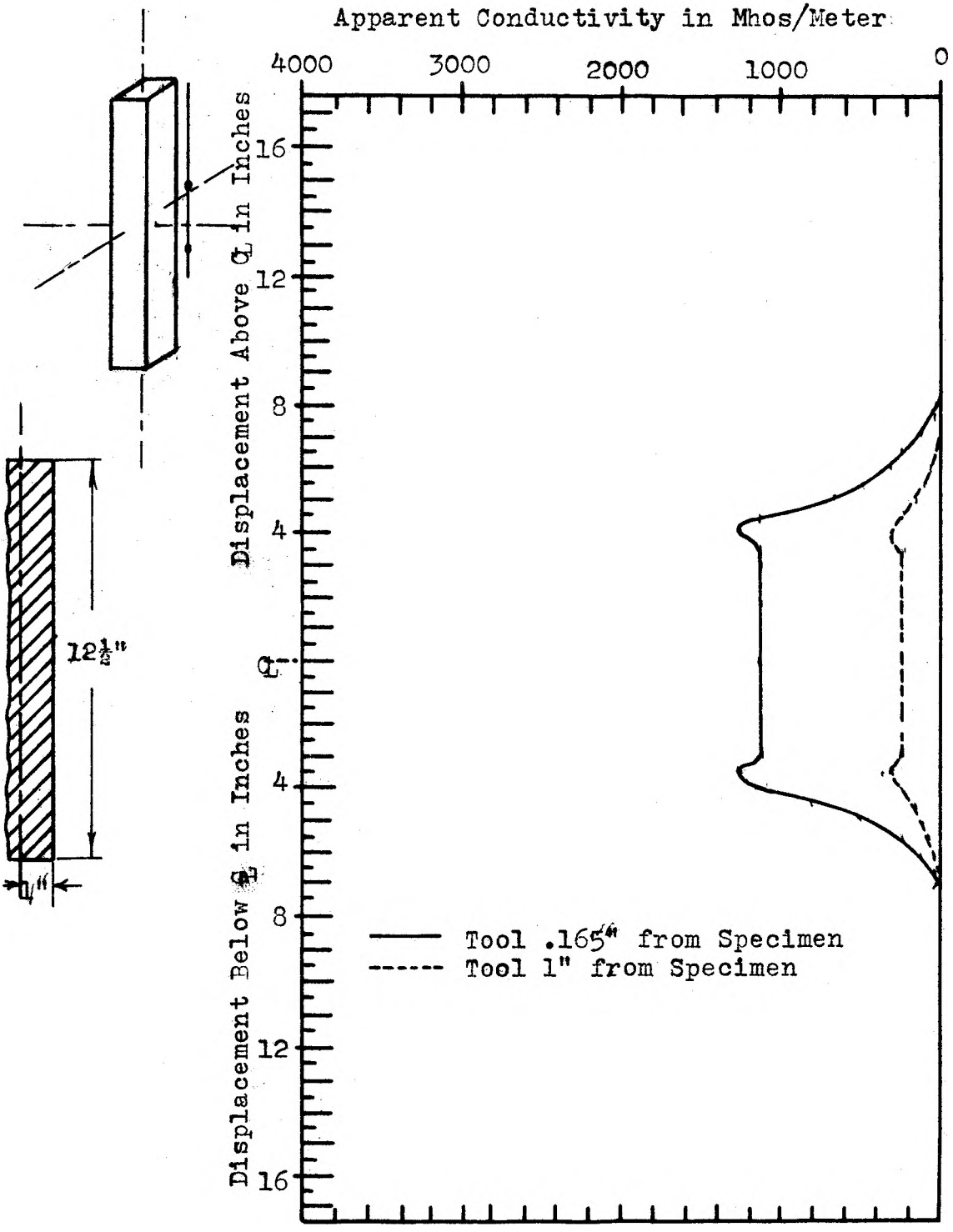

Figure 21. Apparent Conductivity Curves for a 2" x 2" x 12½" Graphite Tetragonal Prism in Air. Tool Parallel to Longitudinal Dimension of 2" x 12½" Face. Curves Uncorrected for Skin Effect.

F. Tetragonal Prism (2" x 2" x 12")

Runs were conducted parallel to the longitudinal axis, parallel to the 2" x 12" face. The curves are illustrated in Figure 21. As will be noticed when the curves of Figure 20 are compared to these, a marked similarity is apparent. It appears that the surface area has a greater influence than the volume of the specimen on the curve values and shapes. The projections on the peaks still seem indicative of the specimen length; i.e., 2/3 of the distance. A maximum radius of investigation of 1-5/8" was obtained for the specimen.

G. Finite Slabs ($\frac{1}{2}$" x $4\frac{1}{4}$" x $7\frac{1}{2}$")

The curves characteristic of a $\frac{1}{2}$" x 4" x $7\frac{1}{2}$" slab, logged parallel to the 4" x $7\frac{1}{2}$" side are depicted in Figure 22. In this case, the peak projections appear to be one-half the length of the specimen. The curve nearest the specimen (tool .165" from specimen) has a high peak value. This may be an indication that the specimen volume is insignificant when compared to the surface area of the side near the tool. As the tool distance increases, the curves appear similar to that of the rhombohedral and tetragonal prisms. Symmetry along a line passed through the specimen centerline is apparent. The maximum radius of investigation for this specimen is 3".

H. Faulted Bodies

Faulted bodies were simulated by displacing the 5" and 4" diameter cylinders, Figure 23; the $\frac{1}{2}$" x 4" x $7\frac{1}{2}$" slabs, Figure 24; and the $3\frac{1}{4}$" diameter cylinders, Figure 25.

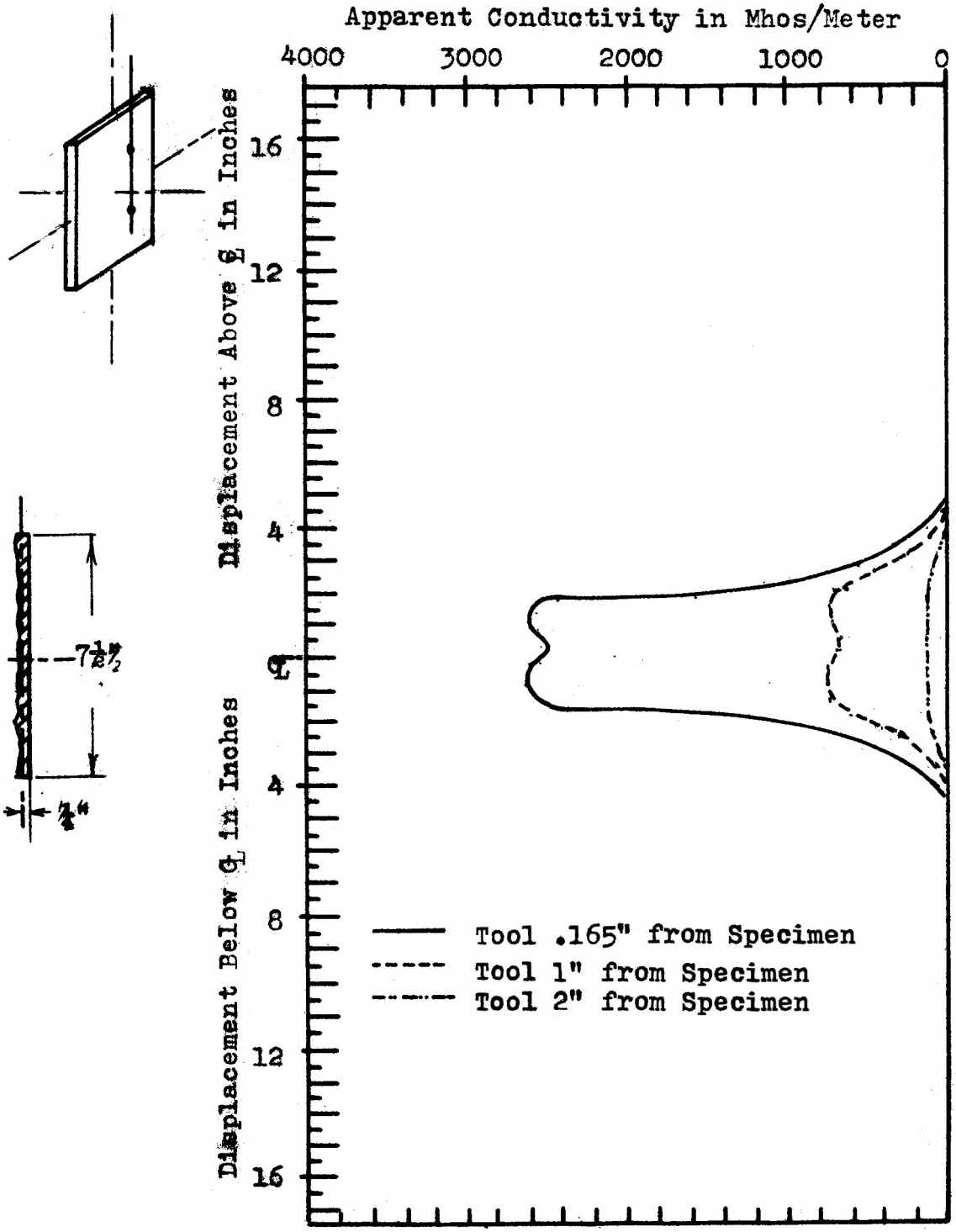

Figure 22. Apparent Conductivity Curves for a ¼" x 4" x 7½" Graphite Slab in Air. Tool Parallel to Longitudinal Dimension of 4" x 7½" Face. Curves Uncorrected for Skin Effect.

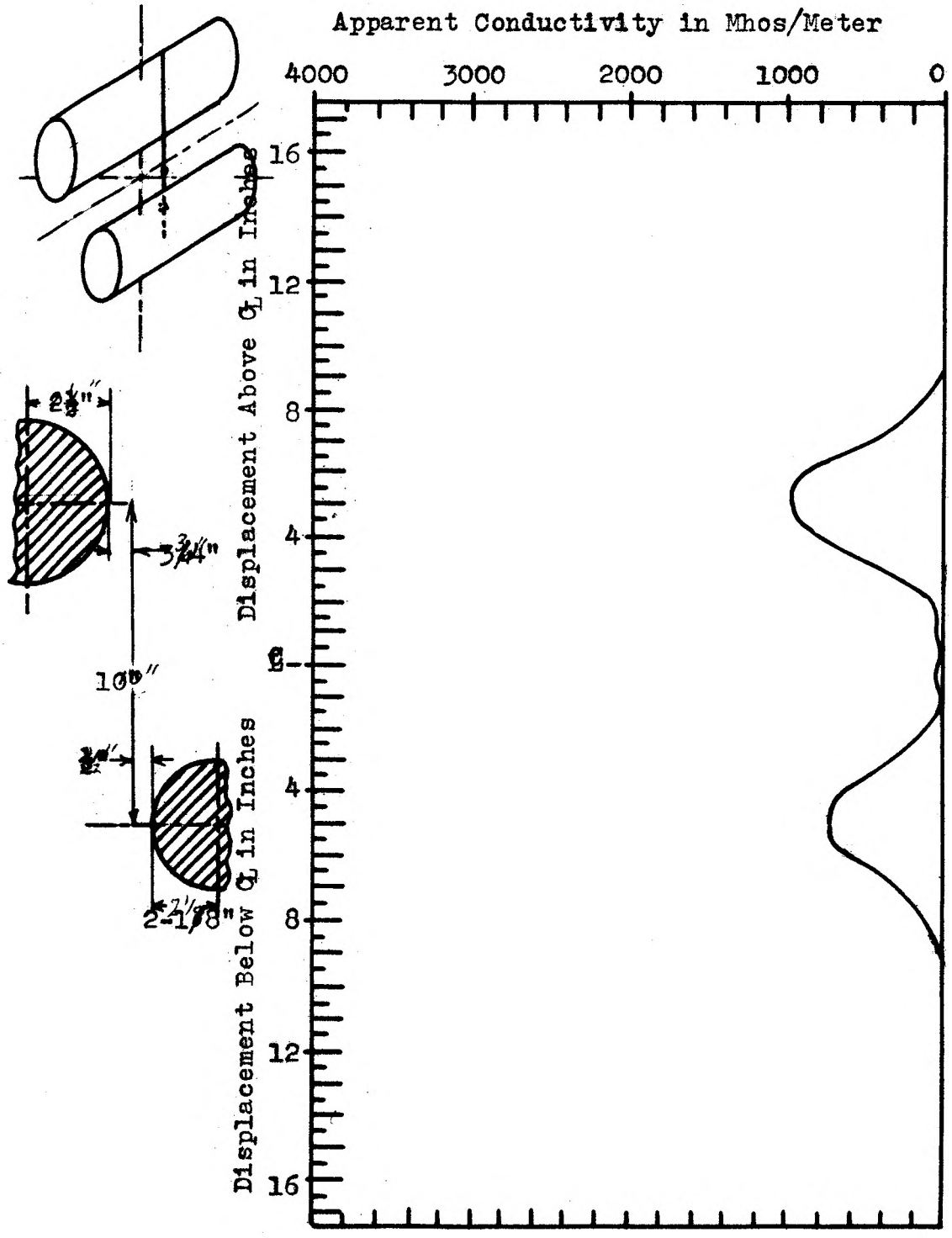

Figure 23. Apparent Conductivity Curve for Two Graphite Cylinders, 5" Diameter and 4¼" Diameter, Displaces 1¼" Laterally and 10" Vertically in Air. Tool Perpendicular to Longitudinal Axis 3/4" from 5" Diameter Cylinder. Curve Uncorrected for Skin Effect.

The 5" and 4" diameter cylinders were displaced 1¼" laterally, and 10" vertically. The tool passed between them, ½" from the 5" diameter cylinder and perpendicular to the longitudinal axis of both cylinders. Analysis of the curve in Figure 23 gives the appearance of two curves, logged separately for the specimens. Each peak, due to its respective cylinder, appears to have symmetry and the characteristic curve of a cylinder. Measurement of the peak to peak distances appears to give the vertical displacement or "throw" of the fault. No maximum radius of investigation was recorded.

Two faulted slabs of ½" x 4" x 7½" each, one located ½" behind the other are depicted in Figure 24. These were logged parallel to the longitudinal dimension of the ½" x 4" x 7½" faces. An examination of the curves shows that the slab behind the closest slab to the tool is "masked". The curve proper, appears to be a distorted version of a curve typical of flat surfaces. However, if the peak to peak distances are measured, it will be found that the displacement of the slab centerline is still approximated.

The curves for a fault having an apparent throw increased by increments, are depicted in Figure 25. Two 3¼"diameter cylinders were initially displaced 2" apart vertically and moved in 1½" increments in a vertical direction. These were logged perpendicular to the longitudinal axis, ½" away from both cylinders. Analysis of the curve shows that a distortion is apparent until the center lines of the cylinder axis are 4½" apart. Then the curves become symmetrical, finally resolving to two separate curves, each characteristic of the

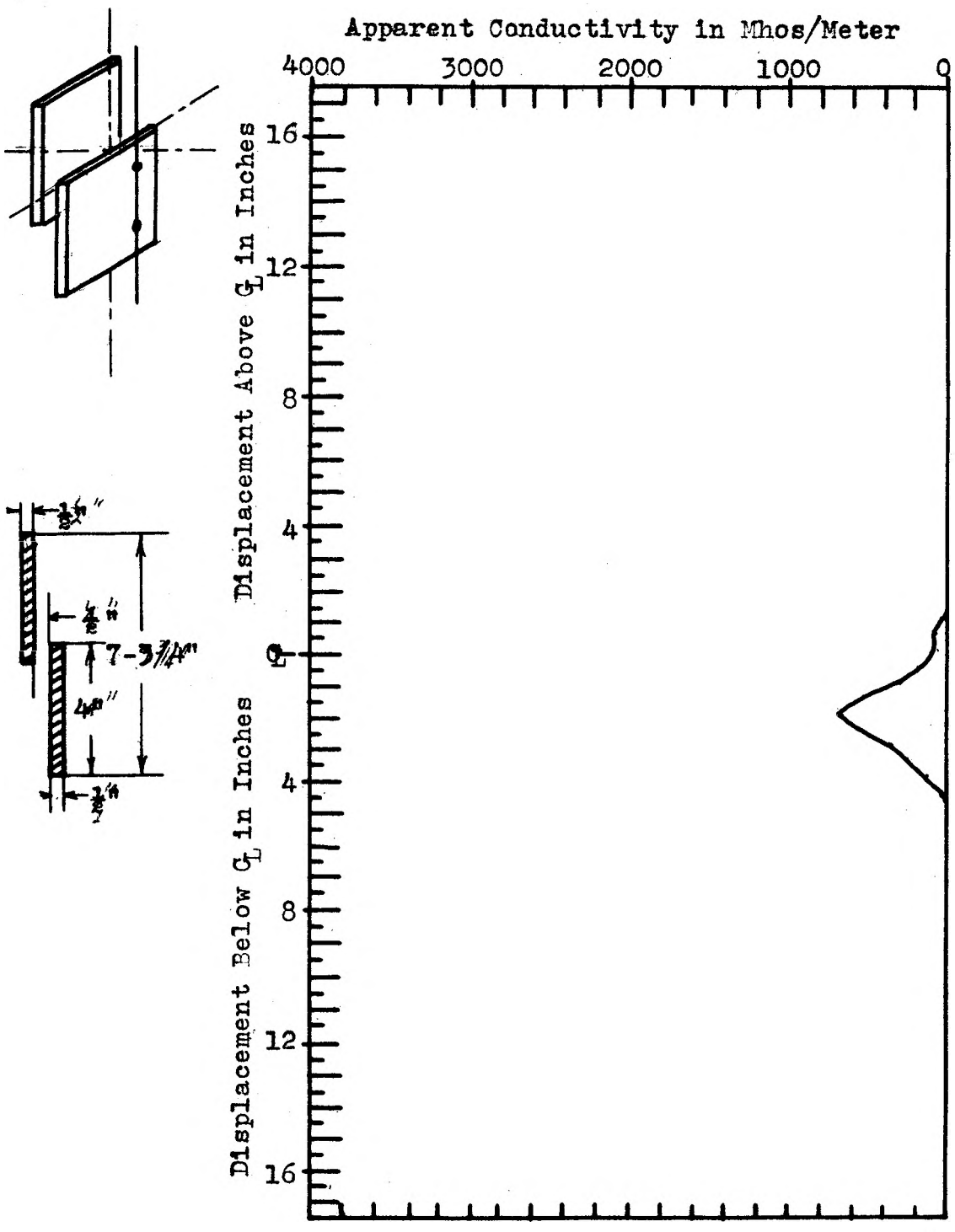

Figure 24. Apparent Conductivity Curve for Two Graphite Slabs, each ½" x 4" x 7½" in Air. Slabs Displaced ½" Laterally and 3-3/4" Vertically. Tool Parallel to 4" x 7½" Face, ½" from Nearest Slab. Curve Uncorrected for Skin Effect.

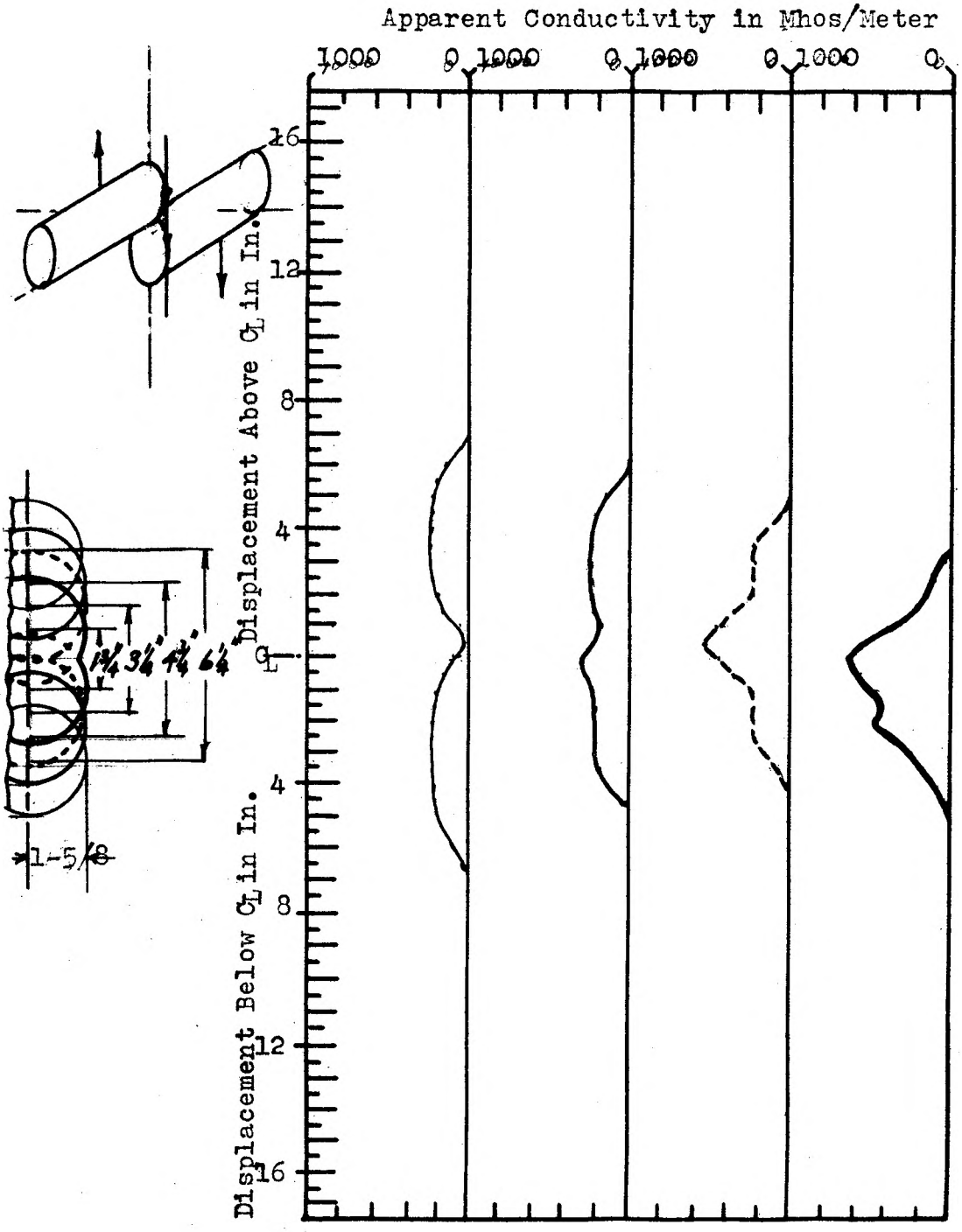

Figure 25. Apparent Conductivity Curve for Two 3½" Diameter Graphite Cylinders, Displaced Vertically by 1½" Increments in Air. Tool Perpendicular to Longitudinal Axis, ½" From Nearest Cylinder. Curves Uncorrected for Skin Effect.

curves given by cylinders. Peak to peak distances, commencing with the distorted curves at a 2" vertical displacement, give a good indication of the apparent fault throw. This becomes more noticeable as the 4" tool spacing is reached and passed. No maximum radius of investigation was recorded.

I. Composite Body

A composite body, composed of a 7-3/4" diameter cylinder, 2" x 4" x 12" orthorhombic prism, two ½" x 21" x 7½" slabs, and the 5" diameter cylinder was logged as depicted in Figure 26. The curves appear to have been modified by the influence of the adjoining bodies, but retain the basic characteristics of their influencing bodies. Beginning at the uppermost portion of the curve, it appears that the first peak is characteristic of a cylinder, passing peak symmetry until the influence of the slabs becomes noticeable. The curve then begins to take the appearance of a flat surface-influenced curve, and finally resolves into a curve typical of a cylinder. With a little study, the reader can correlate the geometric shapes of the curves to the bodies which caused them. No maximum radius of investigation was recorded.

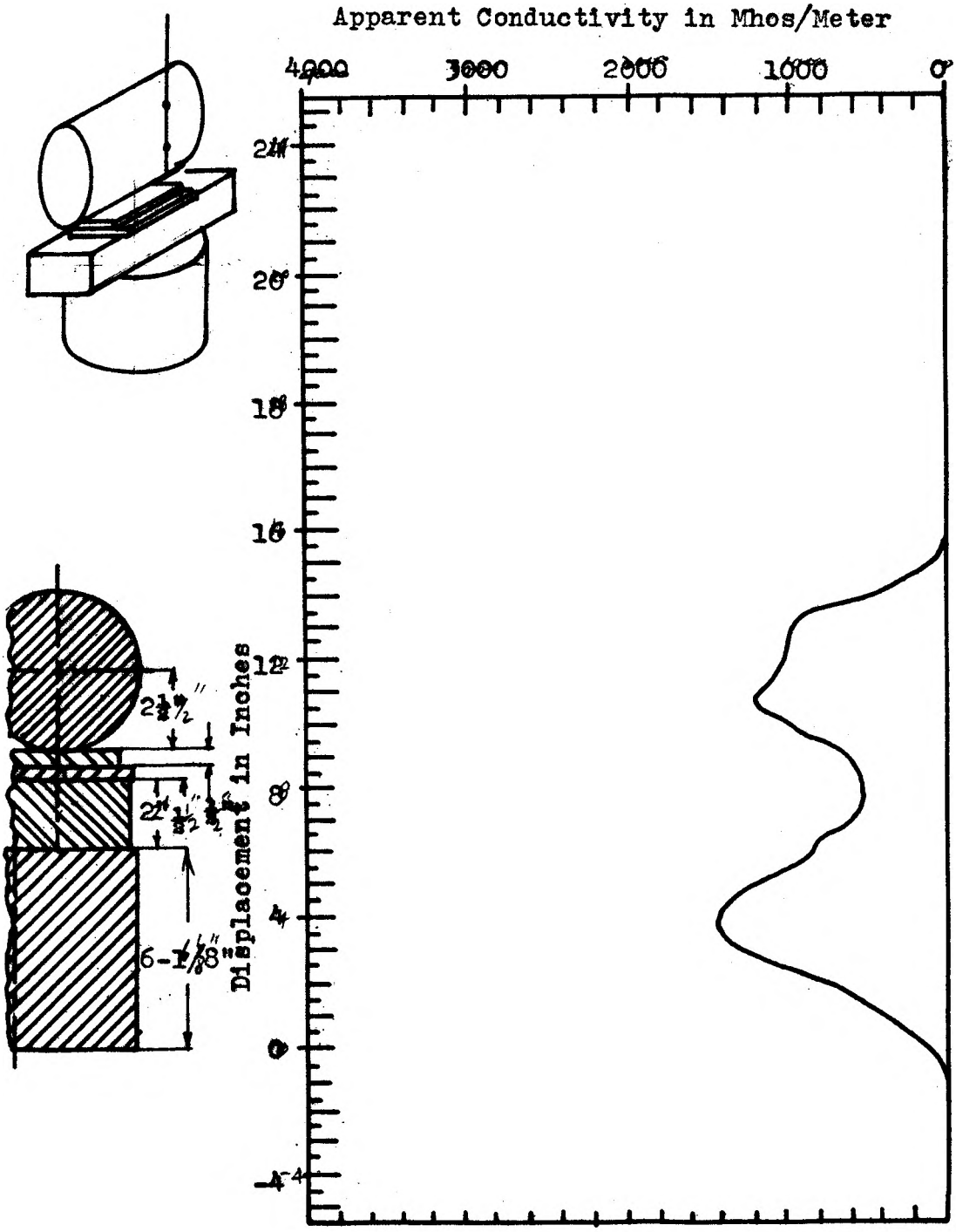

Figure 26. Apparent Conductivity Curve for a Composite Graphite Body in Air. Tool Located ½" from Nearest Projection. Curve Uncorrected for Skin Effect.

VII. CONDUCTIVITY RANGES OF TYPICAL COUNTRY ROCKS

As in other geophysical exploration methods, the induction log is of value to mining exploration only if a detectable conductivity contrast exists between an economically valuable mineral and its surrounding rock. In other words, even though the host or surrounding rock has entirely different physical properties than the mineralization it encloses; if the conductivities are the same, the induction log will fail to detect them. Table II, modified from Jakosky (p. 441) lists typical conductivity ranges of igneous, metamorphic, and sedimentary rocks which may incompass or adjoin the minerals of the conductivity range investigated. The presence of vugs, fissures, and phenocrysts may change the conductivity of the country rock appreciably from one end of the ranges tabulated to the other. Thus, for example, it is highly improbable that two different porphyry copper deposits would have the same conductivity. The table is intended to serve only as a guide; i.e., an indication where induction logging techniques might be advantageously employed.

Rock Type	Resistivity ohm • meters	Conductivity mhos/meter	Scale Conductivity mhos/meter
Basalt	2×10^{4}	5×10^{-5}	5×10^{-2}
Crystalline Rocks	$2\times10^{2}-2\times10^{4}$	$5\times10^{-3}-5\times10^{-5}$	$5 - 5\times10^{-2}$
Diabase	$2\times10^{1}-2\times10^{4}$	$5\times10^{-2}-5\times10^{-5}$	$5\times10^{1}-5\times10^{-2}$
Diorite	5×10^{4}	2×10^{-5}	2×10^{-2}
Gabbro	$1\times10^{2}-1.5\times10^{4}$	$1\times10^{-2}-6.67\times10^{-5}$	$1\times10^{1}-6.67\times10^{-2}$
Gneiss	$2\times10^{2}-3.4\times10^{4}$	$5\times10^{-3}-2.94\times10^{-5}$	$5-2.94\times10^{-2}$
Granite	$3\times10^{-2} - 10^{4}$	$3.33\times10^{-3} - 10^{-4}$	$3.33 - 10^{-1}$
Lava	$1.2\times10^{2}-5\times10^{4}$	$8.33\times10^{-3}-2\times10^{-5}$	$8.33 - 2\times10^{-2}$
Porphry	$6\times10^{1} - 1.5\times10^{4}$	$1.66\times10^{-2}-6.67\times10^{-5}$	$1.66\times10^{1}-6.67\times10^{-2}$
Quartzite	$1\times10^{1}-2\times10^{5}$	$1\times10^{-1}-5\times10^{-6}$	$1\times10^{2}-5\times10^{-3}$
Schist	$5 - 1\times10^{4}$	$2 \times 10^{-1}-1\times10^{-4}$	$2\times10^{2}- 1\times10^{-1}$
Syenite	$1\times10^{2}- 1\times10^{5}$	$1\times10^{-2}- 1\times10^{-5}$	$1\times10^{1}- 1\times10^{-2}$
Trachyte	$1\times10^{1}- 1\times10^{5}$	$1\times10^{-1}- 1\times10^{-5}$	$1\times10^{2}- 1\times10^{-2}$
Clay-Shale	$4\times10^{-4}- 9\times10^{2}$	$2.5\times10^{3}- 1.1\times10^{-3}$	$7.5\times10^{6}- 1.1$
Conglomerate	$2.5\times10^{1}- 1.5\times10^{4}$	$4\times10^{-2}- 6.67\times10^{-5}$	$4\times10^{1}- 6.67\times10^{-2}$
Graywacke	$2\times10^{3}- 1\times10^{4}$	$5\times10^{-4}- 1\times10^{-4}$	$5\times10^{-1}- 1\times10^{-1}$
Limestone	$6\times10^{1}- 5\times10^{5}$	$1.66\times10^{-2}- 2\times10^{-6}$	$1.66\times10^{1}- 2\times10^{-3}$
Sandstone	$3\times10^{1}- 1\times10^{5}$	$3.33\times10^{-6}- 1\times10^{-5}$	$3.33\times10^{1}- 1\times10^{-2}$
Shale	$8 - 1\times10^{4}$	$1.25\times10^{-2}- 1\times10^{-4}$	$1.25\times10^{1}- 1\times10^{-1}$

TABLE II

Conductivity Ranges of Typical Country Rocks Associated with the Minerals Simulated in this Investigation (Modified after Jakosky, 1960)

VIII. CONCLUSIONS

This investigation has brought about the following conclusions and observations:

Orebodies, asymmetrically located in respect to a borehole, and simulated by appropriate materials in a model study, can be detected by induction logging methods.

The curves due to apparent conductivity are indicative of the areal geometry of the model orebodies. This is most noticeable where the surface nearest the tool is curved or flat.

Curve inflection points and projections seem indicative of the longitudinal dimensions of the model orebodies when parallel to the tool. In most cases, a definite ratio between the specimen dimensions and curve inflection points can be established.

Curve inflection points and projections for model orebodies logged perpendicularly to their longitudinal axis are indicative of transverse dimensions only at close tool to specimen distances. As the maximum radius of investigation is approached, this relationship diminishes.

The maximum radius of investigation (MRI) for the model orebodies in air is on the order of 2" to 4". This corresponds to a MRI of 20" to 40" for a full sized orebody logged with a 40" tool in air. The MRI for an orebody in the ground may increase considerably due to the higher conductivity of the latter medium.

For a given model orebody, an estimate of the tool to specimen distance can be determined from analysis of the anomalous curves. As the MRI for a given specimen is approached, this estimate becomes unreliable.

The orientation of model orebodies can be estimated from their curves. This study did not investigate this concept thoroughly enough to yield a definite correlation of curve shape to degrees of dip for a skewed body.

The apparent vertical throw or vertical displacement of a faulted model orebody can be determined from the peak displacements of its curve. The shapes of these peaks are characteristic of the faulted orebody's geometrical shape, if the fault displacement exceeds the coil spacing of the tool.

For a model study using air as an enclosing medium, only conductive orebodies can be investigated. A non-conductive orebody must be placed in a more conductive medium of sufficient dimensions to enclose a maximum percentage of the induced flux.

The conductivity contrasts of the ores and minerals simulated in this study compared to their typical country rocks is indicative of success in the field applications of induction logging methods.

IX. RECOMMENDATIONS

The following recommendations for the study of the applications of induction logging to the detection of orebodies asymmetrically located in respect to a borehole are suggested:

This method should be field tested in a location of known geology. A location having a reasonably homogenous country rock, and a uniform, highly conductive orebody should be chosen. The curves, if applicable, should be checked against those determined by this investigation.

For a model study, the equipment should be as sensitive and stable as technically possible. This is in order to detect minute changes of apparent conductivity which may have a most significant nature. The equipment utilized in this investigation had tendencies to become unstable at the high sensitivity ranges.

Every possible geometrical mode of mineral occurrence should be simulated in order to provide a complete set of reference curves in the event that induction logging becomes a mining exploration tool.

A model study using materials having differing conductivities should be undertaken. This would show the effect of grade percentage variations of minerals and ores on the induction log.

A method should be devised for the model study of minerals and ores having lesser conductivities than their enclosing country or host rocks. This may find application in non-metallic mineral exploration.

A mathematical analysis of the asymmetrical case should be attempted by mathematically competent personnel in an effort to show the reliability of asymmetrical model studies. This may determine quantitative results of known accuracy.

A better understanding of skin effect in an asymmetrical case is needed. A mathematical analysis and model study directed to this end would be of significant value.

X. BIBLIOGRAPHY

Bateman, A. M. (1956) Economic Mineral Deposits, 2nd Ed., John Diley & Sons, New York, N.Y.

Blanchard, J. E. (1957) The Possibilities & Limitations of Geophysical Exploration from Diamond Drill Holes. Seventh Annual Drilling Symposium, University of Minnesota, p. 3-7.

Booyum, B. H. (1957) Schlumberger Electrologging of Small Diameter Drill Holes on the Marquette Range, Michigan. Seventh Annual Drilling Symposium, University of Minnesota, p. 49-54.

Broding, R. A.; Zimmerman, C. W.; Somers, E. V.; Wilhelm, E. S.; and Stripling. A. A. (1952) Magnetic Well Logging. Geophysics Vol. XVII, No. 1.

Broding, R. A. (1957) Radioactive Surveying of Drill Holes. Seventh Annual Drilling Symposium, University of Minnesota.

Clark, A. R. (1956) The Determination of the Long Dimension of Conducting Ore Bodies. Geophysics, Vol. XXI, No. 2, p. 470-477.

De LeMare, G. S. (1959) Long Hole Drilling as an Aid to Mining and Development Work at United Park City Mines Co., AIME Preprint No. 59AU75.

Doll, H. G. (1949) Introduction to Induction Logging and Application to Logging of Wells Drilled with Oil Base Mud. Petroleum Transaction, AIME, June, 1949, T. P. 2641, p. 1-16.

Duesterhoeft, W. D., Jr. (1961) Propagation Effects in Induction Logging. Geophysics Vol. XXVI, No. 2, p. 192-204.

Dumanier, J. L.; Tixier, M. P.; and Martin M.; (1957) Interpretation of the Induction Electrical Log in Fresh Mud. Journal of Petroleum Technology, July 1957.

Guyod, H. (1944) Electric Well Logging. Halliburton Oil Well Cementing Co.

Hallof, P. G. (1957) Drill Hole Electromagnetic Exploration for Sulfide Ores. Seventh Annual Drilling Symposium, University of Minnesota, p. 8-14.

Handbook of Chemistry and Physics (1952) 34th Ed., Chemical Rubber Publishing Co., Cleveland, Ohio, p. 2186, 2200, and 2201.

Heiland, C. A. (1946) Geophysical Exploration. Prentice-Hall, New York, N. Y., p. 763-818.

Jakosky, J. J. (1950) Exploration Geophysics, 2nd Ed., Trija, Newport Beach, California, p. 441. .

McKinstry, H. E. (1959) Mining Geology. Prentice-Hall, Englewood Cliffs, N. J.

Moore, J. E. (1957) Application of Borehole Geophysics to Mining Exploration. Seventh Annual Drilling Symposium, University of Minnesota, p. 26-42.

Prichett, W. C. (1955) A Low Frequency Earth Model. Geophysics, Vol. XX, No. 4, p. 862-864.

Royce, J. (1957) Comparison of Mining Grades with Estimated Grades in Iron Ores, Seventh Annual Drilling Symposium, University of Minnesota.

Schlumberger Document 8. (1958) Introduction to Schlumberger Well Logging. Schlumberger Well Surveying Corporation, p. 37-47.

Seigel, H. O. (1952) Ore Body Size Determination in Electrical Prospecting. Geophysics Vol. XVII, No. 1, p. 907-914.

Smythe, Wm. R. (1950) Static and Dyamic Electricity. 2nd Ed., McGraw Hill, New York, N.Y., p. 318.

Winch, R. P. (1955) Electricity and Magnetism, Prentice-Hall, Englewood Cliffs, N. J. P. 197-244.

Wylie, W. R. J. (1957) The Fundamentals of Electric Log Interpretation, 2nd Ed., Academic Press, New York, N. Y.

Zablocki, C. J.; and Keller, G. V. (1957) Borehole Geophysical Logging Methods in the Lake Superior District. Seventh Annual Drilling Symposium, University of Minnesota, p. 15-24.

Zenor, H. M. (1962) Personal communication.

Zenor, H. M.; and Oshry, H. (1962) Modification of the Geometrical Factor Due to Skin Effect. A paper presented at the Third Annual Meeting of the Society of Professional Well Log Analysts, May 17-18, 1962 in Houston, Texas.

XI. APPENDICES

APPENDIX A

Graphite Specifications

The material utilized for the model orebodies was electrode graphite, manufactured by the Acheson Graphite Division of the National Carbon Company, a division of Union Carbide.

The resistivity specification for Acheson Electrode Graphite is .000813 ohm centimeters.

In terms of conductivities, this would resolve to 1.223×10^5 mhos per meter conductivity.

APPENDIX B

Brine Considerations

A saturated brine solution was mixed from 5 gallons of tap water and sufficient commercial table salt (Morton's fine grain) to provide an excess, at a temperature of 89°F. The salt solution was placed in a plastic tank and its resistivity measured by a standard Wenner configuration utilizing pencil graphite electrodes.

Since $\rho = 2\pi a \frac{V}{I}$ for a Wenner configuration

where ρ = resistivity in ohm meters

a = electrode spacing in meters

$\frac{V}{I}$ = resistance of the medium in ohms

The resistance, $\frac{V}{I}$, was given directly via a megger tester, hooked up expressly for resistivity studies. Then with a 1" electrode spacing, and a .216 ohm resistance reading:

$$\rho = 2 \times 3.1416 \times \frac{1}{39.37} \times .216$$

$$\rho = .0345 \text{ ohm meters}$$

However, since the conductivity is the reciprocal of resistivity, the conductivity σ, of the brine solution is given by

$$\sigma_{brine} = \frac{1}{\rho}$$

$$\sigma_{brine} = \frac{1}{.0345}$$

$$\sigma_{brine} = 29.0 \text{ mhos per meter}$$

The resistivity chart in Schlumberger Document 8 (p. 10) lists a resistivity of .033 ohm meters for a saturated brine solution at a temperature of 89°F.

APPENDIX C

Calibration Considerations

When the tool was placed in the glass tube "borehole" in the brine solution, scale deflections of 1.60, .80, and .25 scale divisions were noted on the .156, .303, and 1 X multipliers respectively.

For the .156 multiplier, this corresponds to a value of $\frac{29}{1.6} = 18.14$ mhos per meter per scale division.

The .303 multiplier converts to a value of $\frac{29}{.80} = 36.30$ mhos per meter per scale division. Similarly, the .25 reading on the 1X multiplier converts to $\frac{29}{.25} = 116$ mhos per meter per scale division. Since the conductivity meter was continually off scale for the .156 and .303 X multiplier setting, the more stable 1X multiplier setting was used. Therefore, converting to terms of the 1X multiplier, the readings on the .156 and .303 multipliers correspond to $\frac{18.14}{.156}$ and $\frac{35.81}{.303}$, or 116 and 117 mhos per meter per scale division respectively. Thus, a reading of .116 mhos per meter per scale division was established for the 1X multiplier setting.

XI. VITA

Robert Walter Piekarz, son of Mr. and Mrs. Walter R. Piekarz was born on March 30, 1935 at Chicopee, Massachusetts. He attended the Chicopee public schools and graduated from the Chicopee High School in June, 1952.

In September, 1952, he entered the Colorado School of Mines. He enlisted in the U. S. Navy in October, 1954, and was graduated from the Class A Fire Control Technician's School, Bainbridge, Maryland as a Fire Control Technician 3rd Class in December, 1955. After serving aboard the USS Knapp and USS Union in the Far East, he was separated as a Fire Control Technician 1st Class in August, 1958.

In September, 1958, he enrolled at the Missouri School of Mines and Metallurgy, and received the B. S. degree in Mining Engineering in January, 1961. During the period of his graduate work, he was employed as a research assistant to Lane Wells Company and as a graduate assistant to the Mining Department. On June 11, 1960, he was united in marriage to Dorothy J. McGlamery of Mexico, Missouri.

He is a member of Sigma Gamma Epsilon, Pi Kappa Alpha, an Associate member of Sigma Xi, a student member in the Society of Exploration Geophysicist and the American Institute of Mining Engineers, and a registered engineer in training for the State of Missouri.

MISSOURI SCHOOL OF MINES & MET.
LIBRARY
104580
OCT 8 1962
ROLLA, MO.